Development of process to transfer large areas of LPCVD graphene from copper foil to a porous support substrate

by

Sean C. O'Hern

Submitted to the Department of Mechanical Engineering
in partial fulfillment of the requirements for the degree of

Master of Science in Mechanical Engineering

at the

MASSACHUSETTS INSTITUTE OF TECHNOLOGY

September 2011

Author .....
Department of Mechanical Engineering
August 11, 2011

Certified by .....
Rohit Karnik
d'Arbeloff Assistant Professor of Mechanical Engineering
Thesis Supervisor

Accepted by .....
David E. Hardt
Graduate Officer, Professor of Mechanical Engineering

Development of process to transfer large areas of LPCVD graphene from copper foil to a porous support substrate

by

Sean C. O'Hern

Submitted to the Department of Mechanical Engineering
on August 11, 2011, in partial fulfillment of the
requirements for the degree of
Master of Science in Mechanical Engineering

Abstract

In this thesis, I present a procedure by which to transfer greater than 25 mm^2 areas of high-quality graphene synthesized via low-pressure chemical vapor deposition from copper foil to porous support substrates. Large-area, high quality graphene on a porous support would serve as a platform by which to create high efficiency porous graphene membranes for use in liquid and gas-phase separation technologies. In this procedure, we transfer greater than 25 mm^2 areas of graphene with few holes and tears to both gold Quantifoil Holey Carbon transmission electron microscope grids with 1.2 μm diameter pores and to Sterlitech polycarbonate track etch membranes with 200 nm diameter pores by bonding the substrates to the graphene then wet-etching the copper. The resulting membrane quality is characterized via Raman spectroscopy, scanning electron microscopy, diffraction patterning, and aberration-corrected scanning transmission electron microscopy.

Thesis Supervisor: Rohit Karnik
Title: d'Arbeloff Assistant Professor of Mechanical Engineering

Acknowledgments

First and foremost, I would like to thank Professor Rohit Karnik for providing direction each step of the way, and all those in the Micro and Nanofluidics Research Group, who patiently answered all my questions, especially Jongho Lee and Tarun Jain, with whom I had many helpful discussions.

I would also like to thank...

...Professor Jing Kong and Dr. Sreekar Bhaviripudi for providing us with graphene and teaching me how to handle the material...

...Professor Evelyn Wang and everyone in the Device Research Laboratory...

...my funding agency, the Center for Clean Water and Clean Energy at MIT and KFUPM, and our collaborators at King Fahd University of Petroleum and Minerals, Professor Tahar Laoui and Professor Motaz Atieh...

...Yong Zhang, Shiahn Chen, and Patrick Boisvert, the research scientists at the Center for the Materials Science and Engineering Electron Microscopy facility, for training me on nearly every instrument in the facility...

...Jiangdong Deng and the Center for Nanoscale Systems at Harvard University for providing access to the Raman microscope...

...Juan-Carlos Idrobo at the Advanced Microscopy Facility at Oak Ridge National Labs and the SHaRE User program for collaborating with me on imaging the graphene...

...all the support staff at MIT, including Thea, Leslie, Joan, and Una...

...my friends at Christ the King Presbyterian for being my home away from home and my family for supporting my decision to return to school.

Above all, I would like to thank my wife Nicole, for her encouragement during the hard times, but more importantly, her willingness to come to a place with such horrible winters. I couldn't have done this without you.

THIS PAGE INTENTIONALLY LEFT BLANK

Contents

1 Introduction **15**

1.1 Motivation: water scarcity 15

1.2 Role of nanostructured materials 17

1.3 Promise of graphene membranes with subnanometer pores 18

1.4 Scope of work 18

2 Background on graphene synthesis and transfer **19**

2.1 Graphene synthesis 19

2.1.1 Mechanical exfoliation 19

2.1.2 Chemical methods 20

2.1.3 Epitaxial growth 21

2.1.4 Chemical vapor deposition 22

2.2 Graphene transfer 24

2.2.1 Mechanically exfoliated graphene transfer 24

2.2.2 Chemically-modified graphene transfer 26

2.2.3 Epitaxial graphene transfer 27

2.2.4 CVD graphene transfer 27

2.2.5 Suspended graphene transfer 28

3 Graphene transfer process **31**

3.1 Selection of graphene source 31

3.2 Transfer of graphene to TEM grids 32

3.2.1 Process 32

3.2.2 Graphene characterization 35
3.3 Transfer of graphene to polycarbonate track etch membranes 40
3.3.1 Process 42
3.3.2 Parameters of transfer and impact on results 44
3.3.3 Second-layer graphene transfer 50
3.3.4 Polycarbonate track etch membrane transfer results 51

4 Conclusions **55**

List of Figures

1-1 Worldwide map of physical and economic water scarcity. Adapted from [1]. 16

2-1 (a) Optical microscope image of graphene on a silicon wafer with a 300 nm thick oxide layer. (b) Atomic force micrograph of single, double, and triple layer graphene. From [2]. Reprinted with permission from AAAS. 20

2-2 (a) SEM image of reduced graphene oxide. (b) Reduction and functionalization of intermediate sodium dodecylbenzenesulfonate (SDBS)-wrapped chemical-modified graphene (CMG) with diazonium salts. (c) TiO_2-graphene hybrid and its proposed response under UV exitation. (d) Chemical route to produce aqueous suspension of reduced graphene oxide. (1) Oxidation of graphite to synthesize graphite oxide (2) Exfoliation of graphene oxide in water by sonication of graphite oxide. (3) Controlled reduction of graphene oxide sheets by hydrazine yielding a colloidal suspension of conductive CMG sheets, which are stabilized by electrostatic repulsion. Reprinted with permission from Macmillian Publishers: Nature Nanotechnology [3], 2009. 21

2-3 (a) Atomic force micrograph of epitaxial graphene (EG) on Si-face 6H-SiC. Inset shows uniform growth over substrate ridges. Height scales are in nm. (b) and (c) display transmission electron microscope image of the cross-section of (a) single-layer and (b) double-layer of EG on Si-face 6H-SiC. First layer of growth is typically not considered graphene since only subsequent growth layers exhibit the unique electronic properties of graphene. Reproduced with permission from [4]. Copyright 2009, the Electrochemical Society. 22

2-4 (a) Temperature and gas flow parameters to synthesize graphene on copper foil via low-pressure chemical vapor deposition. (b) Picture of bare copper foil versus copper foil with synthesized graphene. From [5]. Reprinted with permission from AAAS. 23

2-5 (a) Stamping procedure to transfer pristine graphene to a silicon wafer by using controlled adhesion of polymer layer: (i) Press the patterned stamp onto the highly oriented pyrolytic graphite (HOPG). (ii) The stamp cuts and attaches graphene only the desired pattern. (iii) Inspect the quality of the graphene using microscope. (iii) If the graphene is good, transfer the graphene to the target substrate. Reprinted with permission from [6]. Copyright 2007 American Chemical Society. (b) Stamping procedure to transfer pristine graphene by chemically modifying the surface of the silicon: (i) Modify surface of silicon wafer with perfluorophenylazide (PFPA). (ii) Press HOPG onto surface under 10 psi for 40 min at 140°C. (iii) PFPA covalently bonds to top layer of HOPG, resulting in a covalently-bonded graphene layer on the silicon surface once the HOPG is removed. Reprinted with permission from [7]. Copyright 2009 American Chemical Society. 25

2-6 Polydimethylsiloxane (PDMS) stamping procedure to transfer chemically-modified graphene (CMG) to a silicon wafer. (a) Patterned PDMS stamp is pressed onto a thin layer of CMG. The pressing bonds the CMG to the PDMS stamp and remains on the PDMS stamp when it is pulled away (b). (c) The CMG on the PDMS stamp is then pressed onto the target substrate while heating. The heating releases the PDMS-graphene bond, resulting in a transfer to the target substrate (d). Reprinted with permission from [8]. 26

2-7 (a)LPCVD graphene transfer to Quantifoil Holey Carbon TEM grid. (b) SEM image and TEM image (inset) of transferred graphene on TEM grid. Scale bar is 10 μm. Scale bar in inset is 0.5 μm. Reprinted with permission from [9]. Copyright 2010, American Institute of Physics. 29

2-8 Fabrication of suspended graphene from low-pressure CVD graphene by selective etching of the copper. The top and bottom of each image corresponds to the plan view and side view of the substrate, respectively. (1) CVD synthesized graphene grown on Cu. (2) Graphene from one side of Cu is removed with an oxygen plasma etch, and (3) both sides of the substrate are coated in photoresist. Conventional photolithography is used to pattern the resist on the Cu side of the substrate to (4) expose the mask-defined regions of the Cu. (5) A ferric chloride solution etches the Cu down to the underlying graphene/resist. The remaining photoresist is stripped resulting in (6) a patterned, suspended graphene membrane. Reprinted with permission from [10]. Copyright 2010, American Chemical Society. 30

3-1 LPCVD graphene transferred to Quantifoil Holey Carbon TEM grid via PMMA method imaged in (a) TEM and (b) SEM. (a) TEM image shows defect created in the graphene during transfer process, along with residue from PMMA. (b) SEM image shows large tears in the graphene created during the process. 34

3-2 LPCVD graphene transferred to Quantifoil Holey Carbon TEM grid via direct transfer method imaged in (a) TEM and (b) SEM. (a) TEM image shows clean transfer. (b) SEM image large area coverage with minimal defects. 35
3-3 Four examples of low-quality graphene transfers to TEM grids via Direct Transfer method. 36
3-4 (a) Hypothesis of defect generation in graphene. Nonconformal substrate does not support graphene at all points. This leads to cracks during transfer due to surface tension pulling on unsupported portions of graphene. (b) Graphene dried in critical point drier. Much lower density of cracks as compared to other samples (see Figure 3-3). . . . 37
3-5 Graphene transferred to a TEM grid after final ethanol rinse. Left side of TEM grid in this image was dipped under ethanol, while right side was not. The ethanol wetting the topside of the TEM grid dislodges the amorphous carbon film from the gold grid, resulting in a poor transfer. 38
3-6 (a) Diffraction pattern of sample shows single-layer graphene. (b) Dark field scanning transmission electron microscope (STEM) image of graphene lattice. (c) Dark field STEM image of graphene suspended over pore in Quantifoil Holey Carbon TEM grid. (d) STEM dark field image showing polymer contamination on the surface of the graphene. 40
3-7 (a) Raman spectrum of suspended graphene on TEM grid. High D-band attributed to polymer contamination on the sample. Laser wavelenth was 532 nm. (b) Raman spectrum of suspended graphene on TEM grid transferred without placing in oven. Decreased D-band suggests polymer contamination occurred on the first sample during heating step. 41
3-8 LPCVD graphene transfer process from copper foil to polycarbonate track etched membrane. 43

3-9 (a) Attempted transfer of graphene to polycarbonate track etch membrane (PCTEM) coated with the wetting agent PVP. Water wets surface between graphene and PCTEM completely within 5 s. (b) Transfer of graphene to PCTEM without PVP. Water does not wet surface between graphene and PCTEM. 1" x 3" glass slide is visible in images for reference. 45
3-10 Initial graphene transfer to hydrophobic polycarbonate track etch membrane with 200 nm pores. 46
3-11 Graphene wrinkles on copper created during the contraction of the copper during cooling after graphene synthesis. 47
3-12 Graphene on copper after being exposed to CE-100 copper etchant. Product of reaction is less dense than copper, creating lines of reacted areas with the copper under the graphene. Inset displays crack in graphene formed from strain introduced by the crystals formed from the etching reaction. 48
3-13 Polycarbonate track etch membrane transfer of graphene etched using (a) standard CE-100 etchant (~250 mg/mL $FeCl_3$) concentration at 25°C and (b) dilute, 0.01 g/mL, $FeCl_3 \cdot 6H_2O$ at 45°C. 49
3-14 (a) Graphene on rough copper. (b) Defective lines in the graphene are easily distinguishable on PCTEM. 50
3-15 (a) Arrows point to single pore defects in graphene etched in APS-100 at atmospheric pressure. These result from insolubility of hydrogen nanobubbles created during the etching reaction. (b) Graphene etched in APS-100 under 7 psi increases solubility of hydrogen gas, resulting in few single pore defects. 51
3-16 (a) Single transfer of graphene to polycarbonate track etch membrane. (b) Double transfer of graphene to polycarbonate track etch membranes. 52

3-17 SEM image of double-layer transfer of LPCVD graphene to polycarbonate track etch membrane (PCTEM). Coverage areas displays no large defects over 1 mm^2 area. Inset shows graphene suspended over PCTEM pores. 52
3-18 Sample thresholded image with two defects circled for clarity. Scale bar is 5 μm. Inset is zoomed in image of defect. Scale bar is 1 μm. . . 53

Chapter 1

Introduction

1.1 Motivation: water scarcity

The supply of fresh water in many parts of the world is reaching crisis levels. Currently, 2.3 billion people live in water-stressed areas of the globe. Population growth, exploitation of existing resources, and pollution are expected to drive this number to 3.2 billion by 2025 [11]. These populations constitute over 26 nations, most of which are located in North Africa, the Middle East, eastern Australia, parts of central and south Asia, and southwestern North America (see Figure 1-1). In these regions, lack of water has led to poor human health, hindered economic development, and encouraged geopolitical conflict as the nations compete over limited water supplies [12].

A path to a sustainable freshwater supply must be developed if we wish to maintain our current projection of worldwide development. Improving usage efficiency through technological advances, encouraging conservation and reuse through political policy, and educating the public on efficient water use can have significant impact on water consumption [12]. Additionally, building dams and reservoirs can increase the supply of available water by 10% over 30 years in certain localities [12]. Since 97.5% of all the world's 1.4 billion km^3 of water is contained in the ocean, desalination of seawater has immense potential to impact the water crisis. Contrary to the above approaches that focus on efficient use of existing resources, thereby decreasing the demand, desalination increases the supply. Desalination is already an important

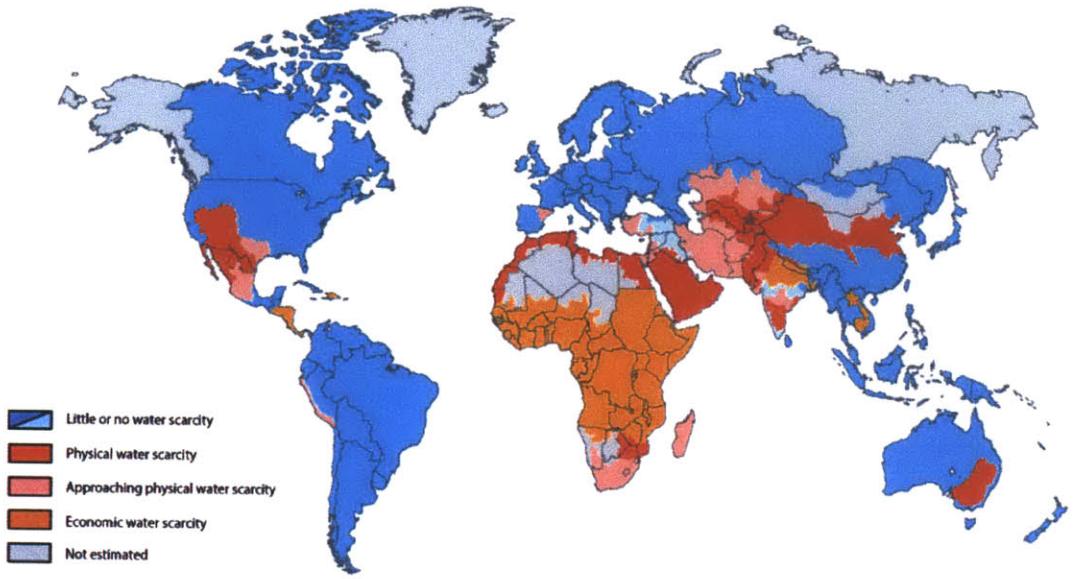

Figure 1-1: Worldwide map of physical and economic water scarcity. Adapted from [1].

water-producing technology in many nations in the Middle East where 52% of all the world's desalinated water is produced [13].

Unfortunately, high energy and capital costs continue to hinder seawater desalination implementation. The minimum thermodynamic limit to produce 1 L of fresh water from seawater is approximately 3-7 kJ, or an order of magnitude greater than the energy required to purify ground or surface water. Additional system inefficiencies increase the actual energy consumption to 10-61 kJ in reverse osmosis (RO) plants and 100-300 kJ in multi-stage flash (MSF) or multi-effect distillation (MED) plants [12]. Including infrastructure, maintenance, and feedwater pretreatment, the cost to produce 1 m^3 of desalinated seawater is between \$0.53-\$1.50 [14]. This makes desalination cost-prohibitive for all but the most advanced nations. If desalination is to be utilized to its fullest extent, including in developing nations, major technological advances must be made to decrease this energy usage requirement.

1.2 Role of nanostructured materials

The increasing demand for fresh water will inevitably encourage the development of new technologies that increase energy efficiency, minimize feedwater pretreatment costs, and decrease capital costs associated with desalination plants. From a technical standpoint, these technologies must focus on: 1) minimizing fouling and scaling on membrane surfaces that decrease RO system performance, 2) minimizing scaling on heat transfer surfaces that decrease MSF/MED system performance, 3) maximizing output of RO membranes and MSF/MED chambers, 4) decreasing the required pressure in RO plants and minimizing the thermal energy required in MSF/MED plants, and 5) optimizing system-level operation of plants [13].

One of the more promising technological advancements that has the potential to address these challenges has been the development of nanostructured materials. Although these materials have been known for several decades, it was only in the past decade that advances in imaging and fabrication have allowed the properties of these materials to be fully understood and manipulated. These materials, which exploit nanoscale phenomena for macroscopic effect, have already been utilized in a variety of disciplines, including drug delivery, energy production, and biosensing [15, 16, 17, 18, 19].

Recently, researchers have begun investigating the use of several different nanostructured materials for water desalination. Carbon aerogels, activated carbon, activated carbon cloth, and carbon nanotubes make excellent electrodes for capacitive deionization due to their intrinsic pores that provide high surface area for electric double layer development. Nanopillars on the surface of MSF/MED condenser tubes can potentially increase heat transfer rates due to dropwise condensation. Zeolite- and carbon nanotubes-based membranes, with their well-ordered, subnanometer-sized pores, have the potential to selectively permit the flow of water while rejecting the flow of salt due to steric hinderance and electrostatic effects at the pore entrance. Each of these are examples of how nanostructured materials could contribute to increasing desalination efficiency [13].

1.3 Promise of graphene membranes with subnanometer pores

Graphene membranes with subnanometer pores are promising nanostructured materials that could potentially have a significant impact on the water crisis. Graphene, a single-layer of sp^2-bonded carbon atoms arranged in a hexagonal lattice, has received significant attention in both the physics field and the electrical engineering field due to its high electron mobility. However, it is the remarkable mechanical properties of graphene, including a breaking strength of 130 GPa [20], an impermeability to helium in its pristine state [21], and the ability to maintain stable subnanometer pores [22, 23], that make it of interest in water desalination. A porous graphene membrane would make a superior desalination membrane because it could withstand the high pressures required in RO plants, permit an extremely high convective flux of water due to its thickness, and reject the flow of salt due to coupled steric and electrostatic effects at the entrance of the angstrom-sized pores. However, such a membrane has yet to be created.

1.4 Scope of work

Realizing the potential of graphene membranes requires methods by which to fabricate large areas of graphene with controlled pores through which molecular or ionic transport can occur. Pores can be generated through a variety of methods [24, 22, 25], but the study of transport through these pores requires large, defect-free areas on a porous support substrate. The goal of this thesis is to develop a process whereby large, defect-free areas of graphene on a porous support substrate can be obtained. Chapter 2 provides a background on current graphene synthesis and transfer techniques, while Chapter 3 outlines the procedure we developed to transfer graphene synthesized via low-pressure chemical vapor deposition from copper foil to porous support substrates.

Chapter 2

Background on graphene synthesis and transfer

Graphene has existed ever since graphite has existed.

- Sean C. O'Hern

2.1 Graphene synthesis

2.1.1 Mechanical exfoliation

Although there is still debate amongst researchers as to when graphene was first isolated, a seminal paper published by Novoselov et al. in 2004 prepared graphene via mechanical exfoliation [2]. This method can then be considered the first graphene synthesis technique. In mechanical exfoliation, scotch tape is pressed onto highly oriented pyrolytic graphite (HOPG) and pulled away. Since the interlayer bonding between graphitic layers is weak, tens to hundreds of graphitic layers pull off the graphite and stick to the scotch tape. The removed layers are then pressed onto a silicon wafer with an oxide layer multiple times. With each pressing, several of the graphitic layers are removed and stick to the wafer. After several presses, few and single-layer graphene eventually adhere to the wafer. Most of these areas are on the order of microns in size or less (see Figure 2-1). Finding the graphene can be a very

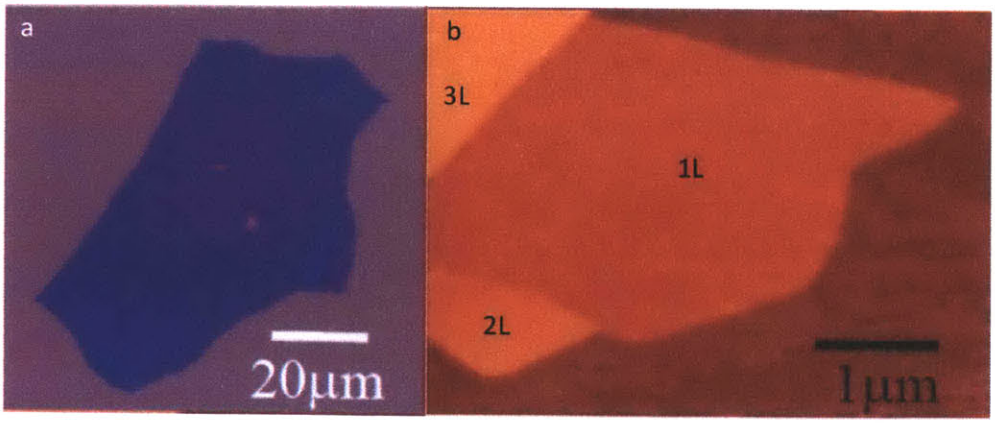

Figure 2-1: (a) Optical microscope image of graphene on a silicon wafer with a 300 nm thick oxide layer. (b) Atomic force micrograph of single, double, and triple layer graphene. From [2]. Reprinted with permission from AAAS.

tedious process. The entire silicon wafer must be scanned in an optical microscope and areas of optical contrast discovered. If such an area exists, the wafer is then taken to an atomic force microscope (AFM), where the number of layers can be determined based on the thickness of the flake. Graphene isolated via mechanical exfoliation still is of the highest quality and therefore very useful for studying the physics of graphene. However, the small areas make it unreasonable for any engineering application.

2.1.2 Chemical methods

Various chemical methods also exist to synthesize graphene by reducing suspensions of graphene oxide (see Figure 2-2). First, graphene oxide is synthesized from graphite by the Brodie, Staudenmaier, or Hummers method [3]. In each of these procedures, the graphite is exposed to strong acids and oxidants. The resulting chemical modification to the graphene structure, which involves the formation of hydroxyl groups, increases the separation distance between the graphitic layers. Sonication following the chemical modification releases the adhesive force between the flakes resulting in a suspension of hydrophillic graphene oxide nanoplatelets. These graphene oxide platelets can then be spincoated on a surface or mixed with a polymer to create thin films or composites. If desired, the graphene oxide can later be reduced to graphene

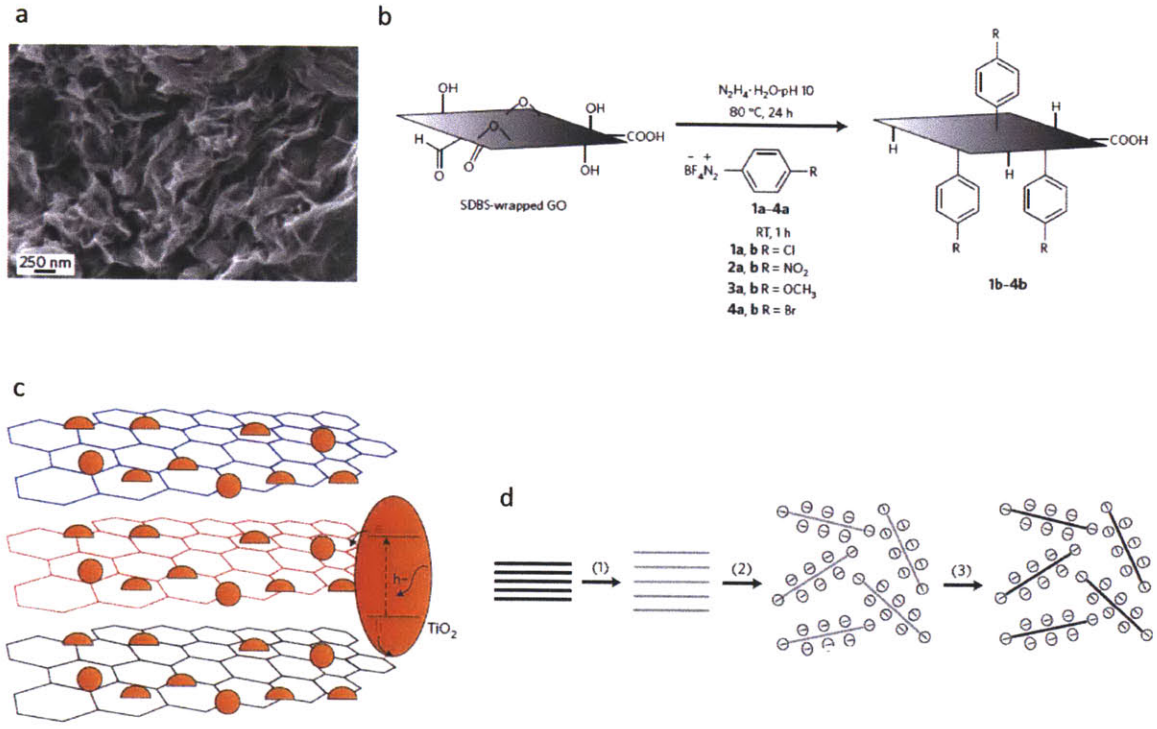

Figure 2-2: (a) SEM image of reduced graphene oxide. (b) Reduction and functionalization of intermediate sodium dodecylbenzenesulfonate (SDBS)-wrapped chemical-modified graphene (CMG) with diazonium salts. (c) TiO_2-graphene hybrid and its proposed response under UV exitation. (d) Chemical route to produce aqueous suspension of reduced graphene oxide. (1) Oxidation of graphite to synthesize graphite oxide (2) Exfoliation of graphene oxide in water by sonication of graphite oxide. (3) Controlled reduction of graphene oxide sheets by hydrazine yielding a colloidal suspension of conductive CMG sheets, which are stabilized by electrostatic repulsion. Reprinted with permission from Macmillian Publishers: Nature Nanotechnology [3], 2009.

via thermal, UV, or chemical methods. This process has been widely used to create graphene "paper" and conductive polymers [3].

2.1.3 Epitaxial growth

Since graphene-based electronics are of considerable interest, the synthesis of graphene on a semiconducting substrate is highly desirable. Epitaxial graphene (EG) grown on a silicon carbide (SiC) wafer is one such method by which to do this and is furthermore compatible with existing industrial wafer technologies. In EG growth, a SiC wafer

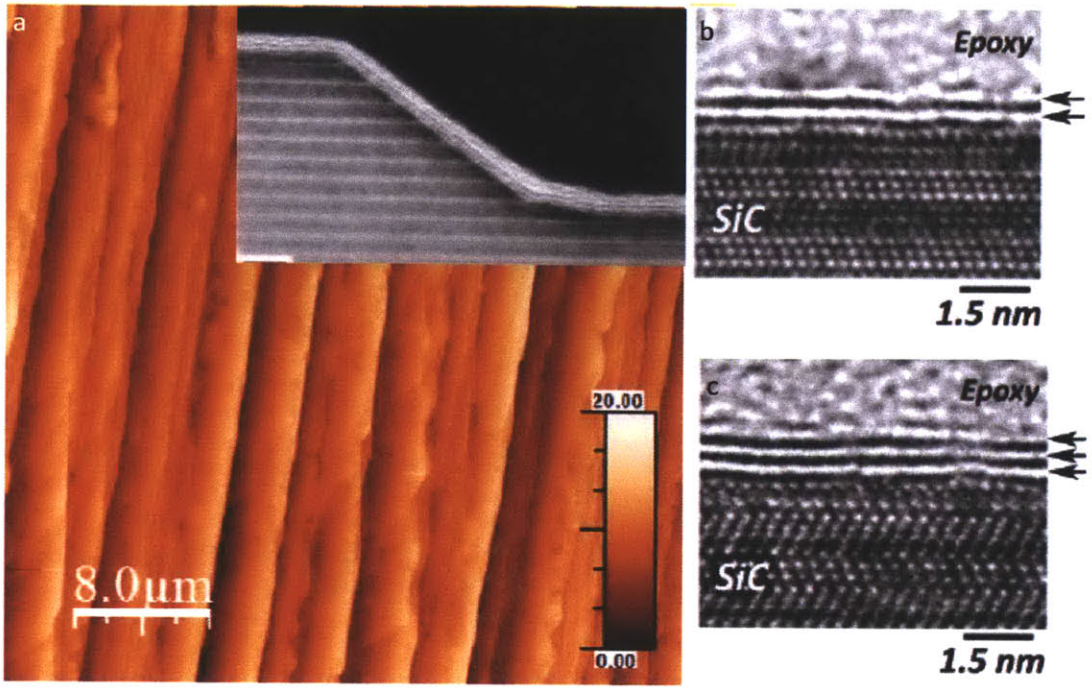

Figure 2-3: (a) Atomic force micrograph of epitaxial graphene (EG) on Si-face 6H-SiC. Inset shows uniform growth over substrate ridges. Height scales are in nm. (b) and (c) display transmission electron microscope image of the cross-section of (a) single-layer and (b) double-layer of EG on Si-face 6H-SiC. First layer of growth is typically not considered graphene since only subsequent growth layers exhibit the unique electronic properties of graphene. Reproduced with permission from [4]. Copyright 2009, the Electrochemical Society.

is heated in ultra-high vacuum to 1200-1700°C. Sublimation of the silicon at this temperature results in a formation of graphene on the surface of the wafer. Figure 2-3a displays an atomic force micrograph of graphene grown over Si-face 6H-SiC. As the inset shows, graphene uniformly coats the steps in the wafer. Figure 2-3b and c show TEM images of single and double-layer EG on Si-face 6H-SiC, respectively. The first layer of growth is typically not considered graphene because only subsequent growth layers exhibit the unique electronic properties of graphene [4, 26, 27, 28, 29].

2.1.4 Chemical vapor deposition

The last graphene synthesis method is graphene synthesized via chemical vapor deposition on a metal catalyst. In 2009, Kim et al. [30] developed a procedure to grow

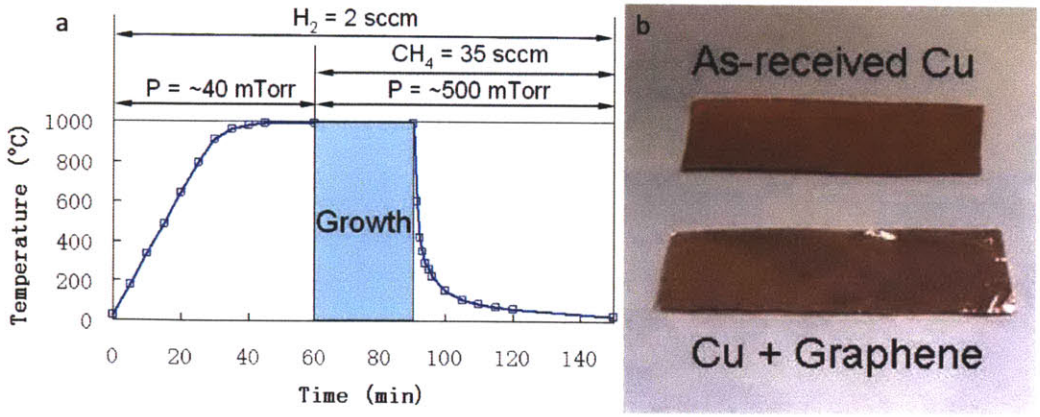

Figure 2-4: (a) Temperature and gas flow parameters to synthesize graphene on copper foil via low-pressure chemical vapor deposition. (b) Picture of bare copper foil versus copper foil with synthesized graphene. From [5]. Reprinted with permission from AAAS.

graphene on a 300 nm-thick nickel film deposited on silicon wafer with an oxide layer by heating the substrate to 1000°C, then flowing methane, argon, and hydrogen over the sample. They were successful in creating few-layer graphene and demonstrating the ability to transfer the graphene to other substrates. Control of the number of layers was listed as one of the primary difficulties with this procedure. Li et al. [5] addressed this issue by growing graphene on another metal catalyst, 25 μm copper foil, at the same temperature of 1000°C but under low pressure (~40 mTorr). Since carbon has low solubility in copper, the growth of the graphene is a self-limiting surface reaction, as opposed to a precipitation process, as it is in nickel. This results in primarily single-layer graphene. Figure 2-4 outlines the temperature and gas flow parameters developed to synthesize graphene via low pressure chemical vapor deposition (LPCVD) and displays an image of the bare copper versus the graphene-coated copper.

2.2 Graphene transfer

For the outstanding properties of graphene to be fully utilized, the synthesized graphene must be able to be transferred to a variety of desirable substrates. This need has led to a host of literature on the transfer of graphene to various substrates for different applications.

2.2.1 Mechanically exfoliated graphene transfer

The transfer of mechanically exfoliated graphene has several unique challenges due to the size of the flake involved in the process. Two separate techniques have shown to be effective in selectively placing mechanically exfoliated graphene on a substrate. In the first method developed by Liang et al. [6], a patterned stamp is fabricated from a silicon wafer with an oxide layer using standard photolithographic techniques. Then a thin polymer layer with controllable adhesion properties is coated over the stamp to act as an adhering layer. When this stamp is pressed on the HOPG, only the patterned area bonds top layer of graphite. When the stamp is removed, only the patterned portion of the stamp brings graphene with it. Then, the stamp-supported graphene is pressed onto the target substrate covered with another adhesive polymer layer. When pulled away, the graphene sticks to the substrate in the desired pattern (see Figure 2-5a).

In another technique, Liu et al. [7] used perfluorophenylazide (PFPA) to chemically modify the surface of a silicon wafer to covalently bond it to graphene. In this process, a silicon wafer with a 300 nm oxide layer is thoroughly cleaned then modified with PFPA, a chemical known to covalently bond to CNTs and fullerenes. The HOPG graphite is then pressed on the PFPA-coated wafer. The PFPA covalently attaches to the top layer of graphite, and when pulled away, removes a single layer of graphene. The covalent bond gives the transferred graphene much more stability. Whereas mechanically exfoliated graphene can be easily removed by rinsing the wafer with a solvent, this graphene can withstand rinsing followed by sonication (see Figure 2-5b).

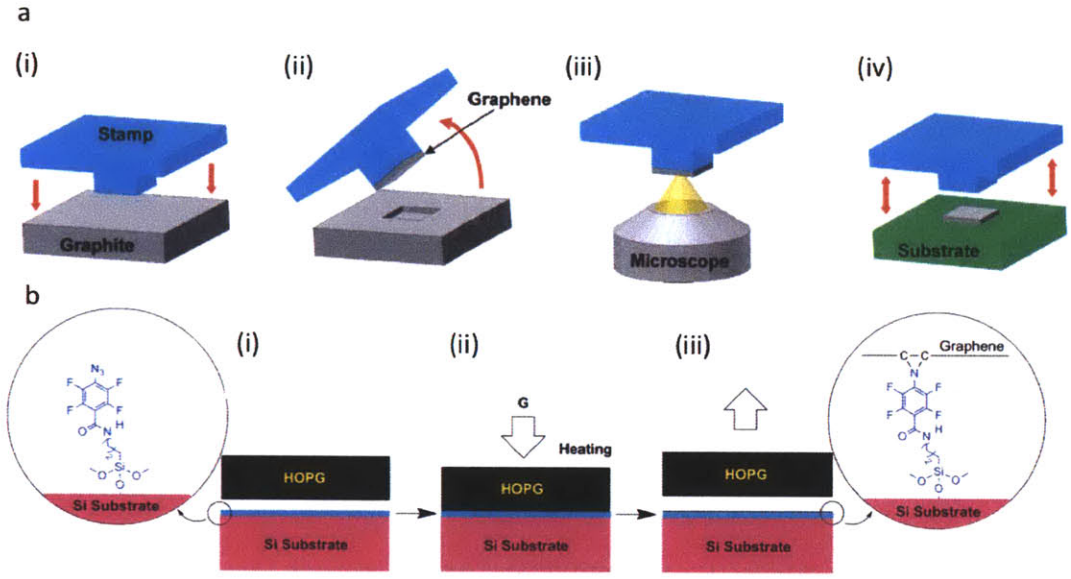

Figure 2-5: (a) Stamping procedure to transfer pristine graphene to a silicon wafer by using controlled adhesion of polymer layer: (i) Press the patterned stamp onto the highly oriented pyrolytic graphite (HOPG). (ii) The stamp cuts and attaches graphene only the desired pattern. (iii) Inspect the quality of the graphene using microscope. (iii) If the graphene is good, transfer the graphene to the target substrate. Reprinted with permission from [6]. Copyright 2007 American Chemical Society. (b) Stamping procedure to transfer pristine graphene by chemically modifying the surface of the silicon: (i) Modify surface of silicon wafer with perfluorophenylazide (PFPA). (ii) Press HOPG onto surface under 10 psi for 40 min at 140°C. (iii) PFPA covalently bonds to top layer of HOPG, resulting in a covalently-bonded graphene layer on the silicon surface once the HOPG is removed. Reprinted with permission from [7]. Copyright 2009 American Chemical Society.

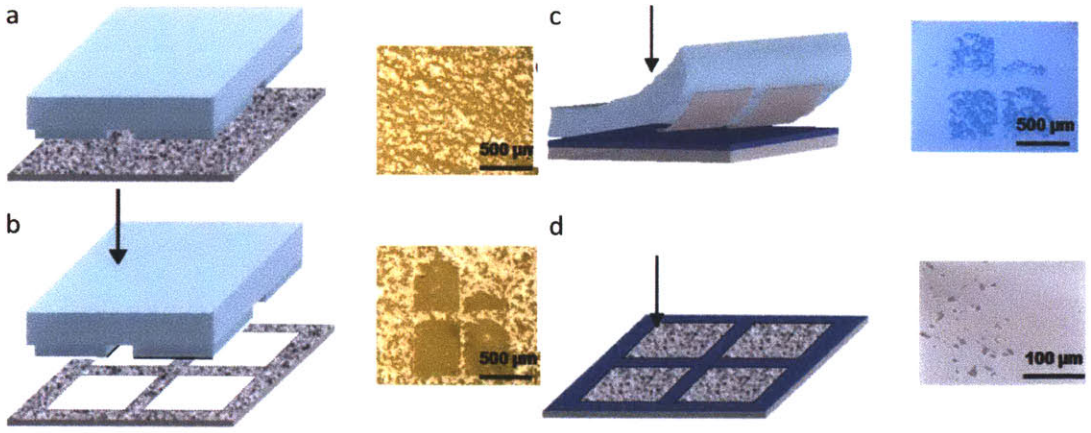

Figure 2-6: Polydimethylsiloxane (PDMS) stamping procedure to transfer chemically-modified graphene (CMG) to a silicon wafer. (a) Patterned PDMS stamp is pressed onto a thin layer of CMG. The pressing bonds the CMG to the PDMS stamp and remains on the PDMS stamp when it is pulled away (b). (c) The CMG on the PDMS stamp is then pressed onto the target substrate while heating. The heating releases the PDMS-graphene bond, resulting in a transfer to the target substrate (d). Reprinted with permission from [8].

2.2.2 Chemically-modified graphene transfer

The transfer of reduced graphene oxide is similar to that of pristine graphene. Allen et al. [8] developed procedure to transfer selected areas of CMG spincoated into a thin film on a glass slide to a silicon wafer using a patterned polydimethylsiloxane (PDMS) stamp. After synthesizing the CMG and suspending it in solution, the CMG is spincoated into a thin film on a glass slide. The speed of operation determines the thickness of the CMG layer. After drying, a patterned PDMS stamp is pressed onto the dried CMG layer. The CMG adheres more strongly to the PDMS than it does to the glass slide, and therefore transfers to the PDMS when the stamp is lifted. The PDMS stamp can then be pressed onto a silicon wafer and heated for 30 min at 75°C. The heating releases the adhesion between the PDMS and the graphene due to the dissociation of low molecular weight oligomers on the surface. When the PDMS is lifted, the graphene remains (see Figure 2-6).

2.2.3 Epitaxial graphene transfer

Epitaxial graphene is especially difficult to transfer due to the resistance of SiC to chemical etching. Caldwell et al. [31], however, developed a dry transfer technique using thermal release tape purchased commercially from Nikko Dento. In their procedure, the graphene is synthesized on SiC as described above. Then, thermal release tape is pressed onto the graphene. When removed, the tape brings with it the graphene layer. The tape-supported graphene is then pressed on a silicon wafer, bonding the graphene to the wafer. After heating the device to a few degrees above the 120°C release temperature, the tape can be easily removed while the graphene remains on the wafer. Lastly, to clean the polymer residue from the graphene surface, the sample is dipped in a toluene, acetone, methanol solution for several minutes at room temperature. The result is a large area transfer with few defects. The process can be repeated for a second, third, and fourth time to increase the coverage of the graphene and the number of layers of graphene.

2.2.4 CVD graphene transfer

The primary technique to transfer CVD graphene to an arbitrary substrate was developed by Reina et al. in 2009 [32]. Reina et al. first spincoated and cured a 1 μm layer of polymethyl(methyl) acrylate (PMMA) on the as-synthesized graphene to use a sacrificial support layer before etching the nickel in a ~3% vol. HCl bath. After etching, the PMMA-supported graphene was then placed on the arbitrary support and permitted to air dry. After drying, the PMMA was dissolved in an acetone bath.

This method has been used to fabricate graphene areas greater than 1 cm^2 on a variety of substrates. However, residual PMMA on the surface of the graphene after PMMA removal degrades the quality of the graphene. To address this issue, several groups began using polycarbonate (PC) as a sacrificial support layer as opposed to the PMMA. PC dissolves much cleaner in chloroform than PMMA in acetone, thereby leaving very little residue [33].

2.2.5 Suspended graphene transfer

Because graphene is a two dimensional material, its properties can be greatly influenced by the supporting substrate. Consequently, it is highly desirable to create suspended graphene sheets. Some of the most useful porous substrates for suspension are TEM grids. A TEM grid-supported graphene film can be placed directly in a TEM and investigated through high resolution imaging, diffraction patterning, and electron energy loss spectroscopy. Additionally, a graphene-based TEM grid is beneficial as a standalone commercial product due to its low background noise. Therefore, several different groups have created TEM-supported graphene sheets by various methods.

The first transfer of graphene to a TEM grid was performed by Regan et al. in 2010 [9]. Regan et al. directly transferred graphene to a Quantifoil Holey Carbon TEM grid with 1.2 μm holes by placing the TEM grid on the as-synthesized LPCVD graphene and placing on it a drop of isopropanol (IPA). The IPA fills in the gaps between the TEM grid and the graphene and as it evaporates, draws the two into contact. Then they placed the the sample in a 0.1 g/mL $FeCl_3$ bath for 2 h to etch away the copper. After rinsing, the TEM-supported transfer was complete (see Figure 2-7). Pantelic et al. [34] developed a similar procedure, except they used chloroform as the bonding solvent and applied formvar as an additional support during the removal of the copper (later dissolved in chloroform). They displayed the benefit of a graphene TEM grid by imaging DNA deposited on their graphene TEM grid.

Commercially-available graphene TEM grids are now available for purchase from Graphene Supermarket. Although the technology is not disclosed, the method by which Graphene Supermarket creates their membranes appears to be similar to the method described by Aleman et al. [10]. In this process, the supporting substrate is the copper itself. After synthesizing the graphene on copper, a photoresist is spincoated onto the graphene. Selected areas of the resist are exposed to UV light via masking, then developed. After rinsing away the developed resist, the exposed copper is etched in a 0.1 g/mL $FeCl_3$ bath. The result is graphene suspended over copper (see Figure 2-8).

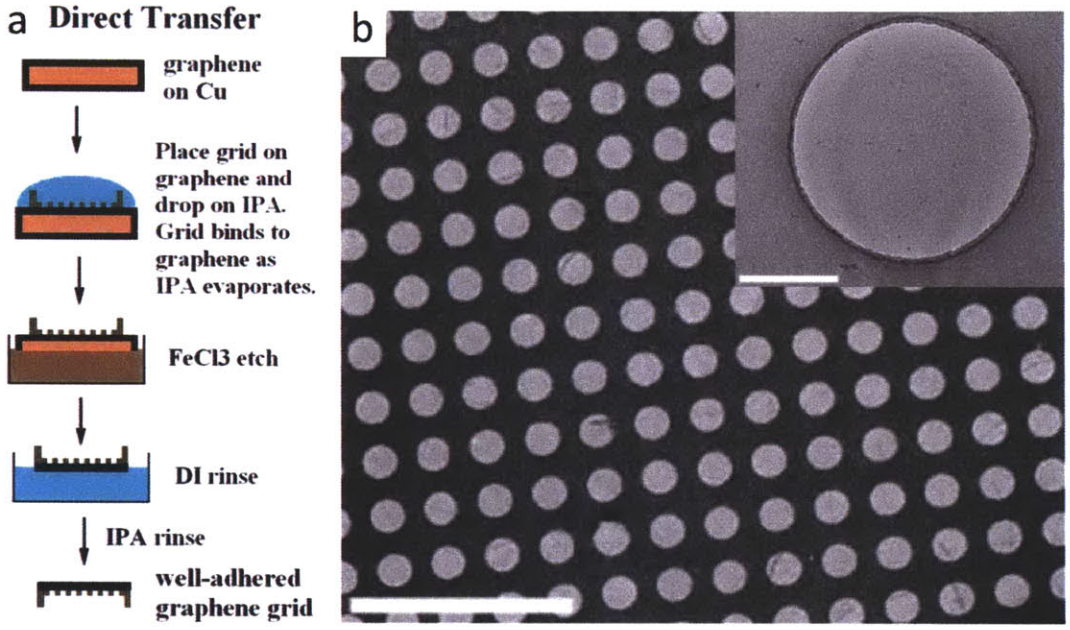

Figure 2-7: (a)LPCVD graphene transfer to Quantifoil Holey Carbon TEM grid. (b) SEM image and TEM image (inset) of transferred graphene on TEM grid. Scale bar is 10 μm. Scale bar in inset is 0.5 μm. Reprinted with permission from [9]. Copyright 2010, American Institute of Physics.

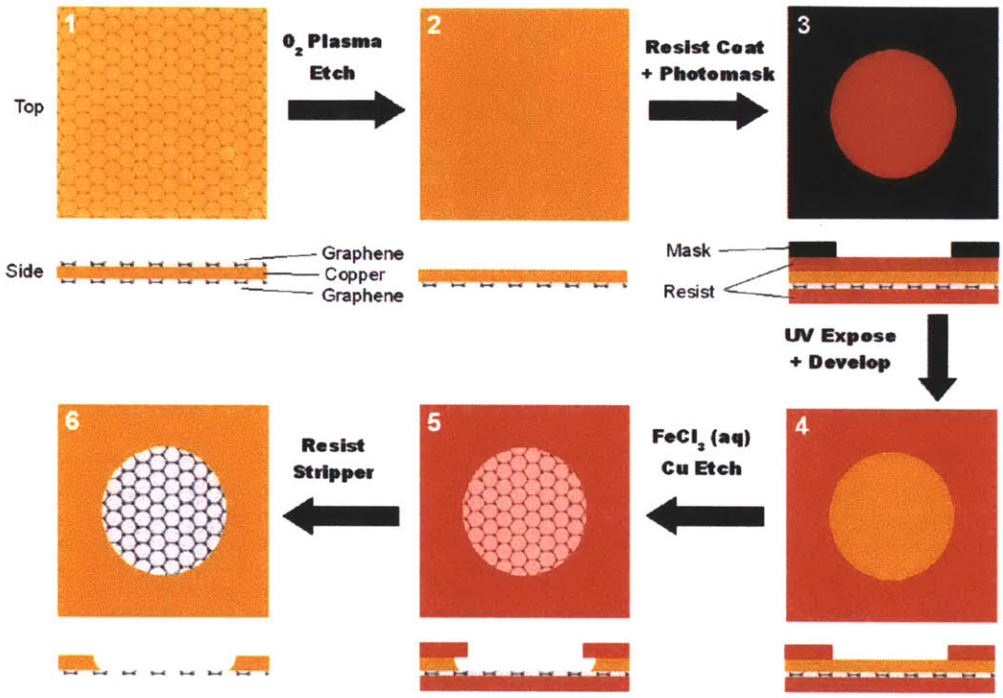

Figure 2-8: Fabrication of suspended graphene from low-pressure CVD graphene by selective etching of the copper. The top and bottom of each image corresponds to the plan view and side view of the substrate, respectively. (1) CVD synthesized graphene grown on Cu. (2) Graphene from one side of Cu is removed with an oxygen plasma etch, and (3) both sides of the substrate are coated in photoresist. Conventional photolithography is used to pattern the resist on the Cu side of the substrate to (4) expose the mask-defined regions of the Cu. (5) A ferric chloride solution etches the Cu down to the underlying graphene/resist. The remaining photoresist is stripped resulting in (6) a patterned, suspended graphene membrane. Reprinted with permission from [10]. Copyright 2010, American Chemical Society.

Chapter 3

Graphene transfer process

Building upon the foundation of the transfer processes listed in Chapter 2, we developed a procedure to transfer graphene to two different porous support substrates: Quantifoil Holey Carbon transmission electron microscope (TEM) grids and Sterlitech polycarbonate track etch membranes (PCTEM).

3.1 Selection of graphene source

In order to optimize membrane area, an estimate of the expected flow rate of water through subnanometer pores in graphene had to be calculated. Suk et al. [35] performed molecular dynamic simulations of water flow through both 0.75 nm pores and 2.75 nm pores in graphene. The group reported a molecular velocity of 10 molecules/ns through the 0.75 nm pore under 100 MPa. Assuming linear dependence of flow rate on pressure, the resistance of water through graphene is then

$$R = \frac{\Delta P}{Q} = \frac{100 MPa}{10 molecules/ns} = 5.6 \times 10^5 \mu m^2 * min * bar/\mu L$$

assuming 1×10^{12} pores/cm^2 in the graphene and a substrate porosity of 10%. If the minimum expected flow measurement capability is 0.01 μL/min, and the applied

pressure is 0.5 bar, then the area required is

$$A = \frac{Q * R}{\Delta P} = \frac{0.01\mu L/min * 0.5bar * 5.6 \times 10^5 \mu m^2 * min * bar/\mu L}{0.5bar} = 1.12mm^2 \approx 1mm^2$$

Therefore, the required graphene area must be on the order of 1 mm^2. This constraint immediately discards mechanically exfoilated graphene as a source, as the largest areas are on the order of square microns. Although epitaxial graphene is of very high quality, it is difficult to synthesize and transfer. Therefore LPCVD graphene was selected as the optimum graphene source. In order to secure this graphene source, we collaborated with Prof. Jing Kong (MIT Electrical Engineering and Computer Science Department) and Dr. Sreekar Bhaviripudi (MIT Materials Science and Engineering Department), who graciously provided us with LPCVD graphene synthesized in their lab.

3.2 Transfer of graphene to TEM grids

3.2.1 Process

Graphene preparation

Graphene coats both sides of the copper foil when synthesized via LPCVD. To reduce the occurrence of defects during the transfer process, the graphene on one side of the copper foil must be removed. This was accomplished by first etching the backside of the copper for 10 min then rinsing in DI water for 10 min. After the rinse, the copper-supported graphene was submerged fully in the DI water. The surface tension from the dipping procedure pulls loose graphene from the backside of the copper. An additional 5 min etch further dislodges the unwanted graphene, followed by another DI water rinse. The remaining copper is approximately 5 μm thick with very little graphene on the backside.

PMMA transfer process

As discussed in Chapter 2, graphene transferred to a porous TEM grid is easy to characterize via TEM imaging, electron energy loss spectroscopy, diffraction patterning, and Raman spectroscopy. Therefore, we selected a gold Quantifoil Holey Carbon TEM grid with 1.2 μm holes as the first substrate upon which to transfer LPCVD graphene and did so via a modified version of the PMMA transfer method developed by Reina et al. [32]. Briefly, after preparing the graphene as described above, the as-synthesized graphene on copper was spincoated with a thin layer of polymethyl(methyl) acrylate (PMMA) (1 min at 2500 RPM to produce a $\sim$2 μm layer). Afterwards, the sample was baked in an oven at 120°C for 5 min to cure the polymer support. To ensure proper etching of the copper, after curing, the backside of the copper was cleaned with acetone and the edges of the copper removed. The sample was then floated on the surface of CE-100 copper etchant (active etchant is $FeCl_3$, commercially available from Transene) and etched for 60 min. To rinse the graphene after etching, the sample was removed from the etchant and placed in two subsequent DI water baths for 10 min each. Lastly, the now PMMA-supported graphene was scooped onto the TEM grid, air-dried, then heated in a quartz-tube furnace under 700 sccm hydrogen and 300 sccm argon at 450°C under atmospheric pressure for 90 min to remove the PMMA. The results of the transfer are shown in Figure 3-1.

As shown in Figure 3-1, the transferred graphene was of very low quality. First, it had many tears and holes which we attributed to the heating of the TEM and graphene sample to during the annealing process. Second, pyrolysis of PMMA leaves significant residue on the surface, thereby decreasing the quality of the graphene.

Direct transfer procedure

To improve the quality of the transfer, we next followed the "Direct Transfer" procedure developed by Regan et al. [9]. Briefly, a TEM grid was positioned on top of the as-synthesized and prepared graphene. Then, a drop of isopropyl alcohol (IPA) was placed on top of the TEM grid and the as-synthesized graphene. The IPA wets the

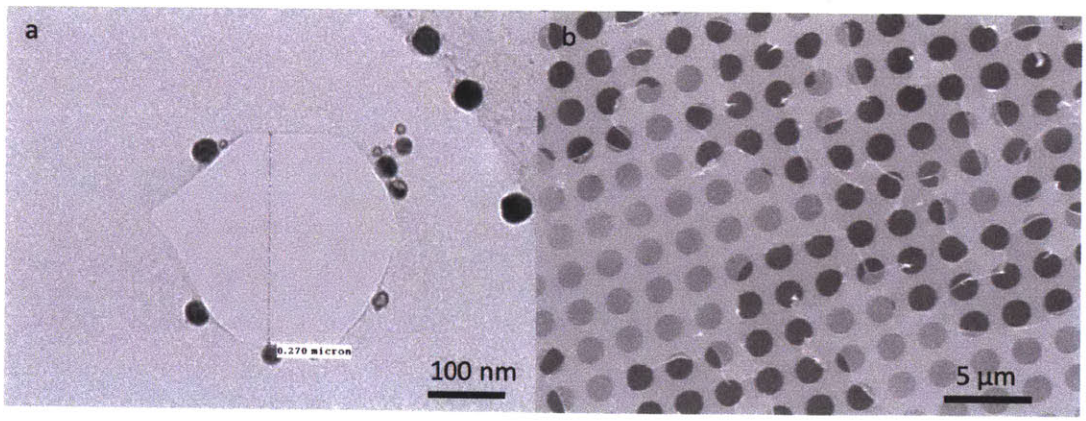

Figure 3-1: LPCVD graphene transferred to Quantifoil Holey Carbon TEM grid via PMMA method imaged in (a) TEM and (b) SEM. (a) TEM image shows defect created in the graphene during transfer process, along with residue from PMMA. (b) SEM image shows large tears in the graphene created during the process.

gap between the amorphous carbon thin film on the TEM grid and the graphene. As the IPA exits this gap through evaporation, the flexible amorphous thin film draws into conformal contact with the graphene. This contact results in significant adhesion force between the TEM grid and the graphene. After air drying, the sample was heated in an oven at 140°C for 10 min to enhance adhesion, then floated on the surface of CE-100 copper etchant and etched for 60 min as before (later, we switched to using APS-100 for reasons discussed in 3.3.2). Lastly, the TEM grid was scooped from the etchant and rinsed in two subsequent DI water baths then air-dried. Figure 3-2 displays the results of the transfer. As shown, we were able to transfer over 2500 μm^2 of clean graphene with a coverage quality greater than 99%.

Unfortunately, this transfer technique had very low yield; about 1 in 20 resulted in a high-quality transfer (see Figure 3-3). We hypothesized that the defects were being generated because the amorphous carbon film on the TEM grid did not conform to all the ridges in the as-synthesized graphene. After the copper was etched, any unsupported graphene floated free. As it dried, surface tension from the water pulled on loose portion of the graphene and created the tears. To test this theory, we dried the sample using a critical point dryer (CPD). The CPD dries the sample without the graphene experiencing the surface of a liquid as it dries. As seen from Figure 3-4,

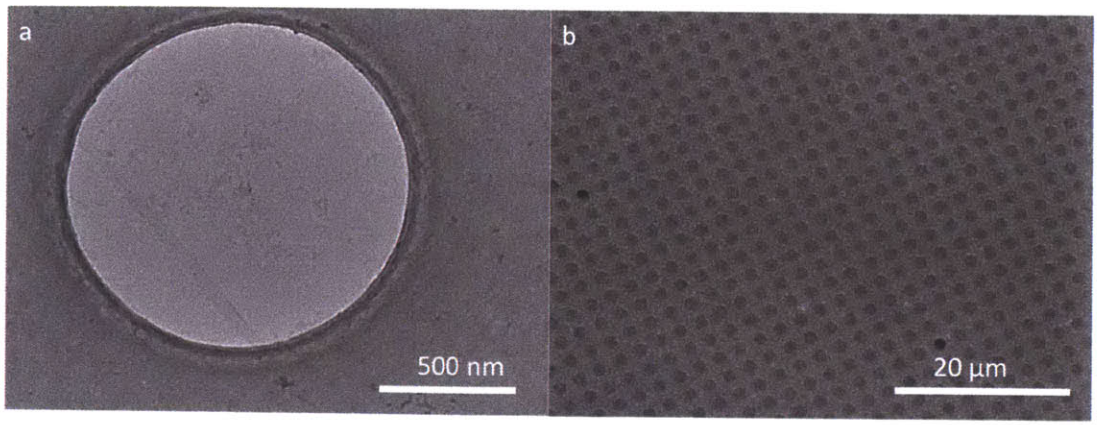

Figure 3-2: LPCVD graphene transferred to Quantifoil Holey Carbon TEM grid via direct transfer method imaged in (a) TEM and (b) SEM. (a) TEM image shows clean transfer. (b) SEM image large area coverage with minimal defects.

the graphene coverage quality was much higher than previously reported, supporting our hypothesis.

Improved direct transfer procedure

Since surface tension during the drying process was a determining step in the quality of the transfer, we selected to rinse the graphene in ethanol after the DI water baths, since at room temperature the surface tension of ethanol is about 33% that of DI water (0.022 N/m for ethanol to 0.072 N/m for DI water). The reduced surface tension also means that the sample will no longer float on the surface, so the TEM grid must be manually held at the surface. If a portion of the TEM grid dips into the ethanol, then the ethanol will wet the surface of the amorphous carbon film and dislodge the film from the gold TEM grid. Figure 3-5 is an example of a TEM-grid supported graphene in which a portion of the TEM grid was dipped in the ethanol. The dipped portion is clearly distinguishable from the portion not dipped.

3.2.2 Graphene characterization

After transfer to the TEM grid, the graphene quality was characterized via diffraction patterning, aberration-corrected scanning transmission electron microscope (STEM)

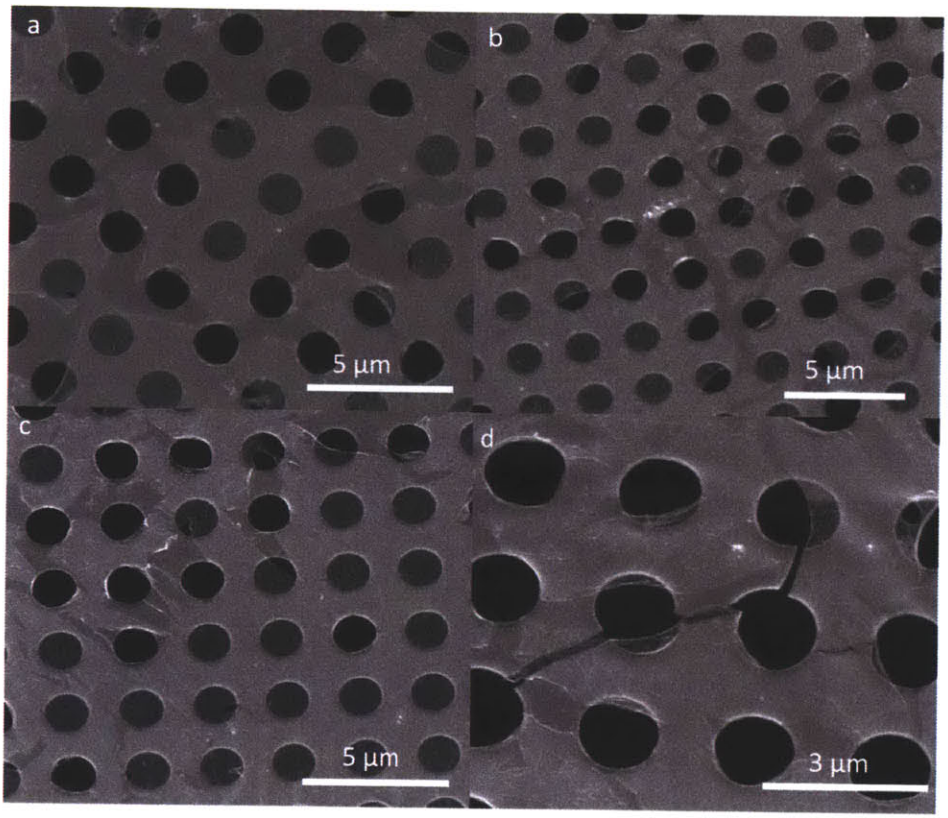

Figure 3-3: Four examples of low-quality graphene transfers to TEM grids via Direct Transfer method.

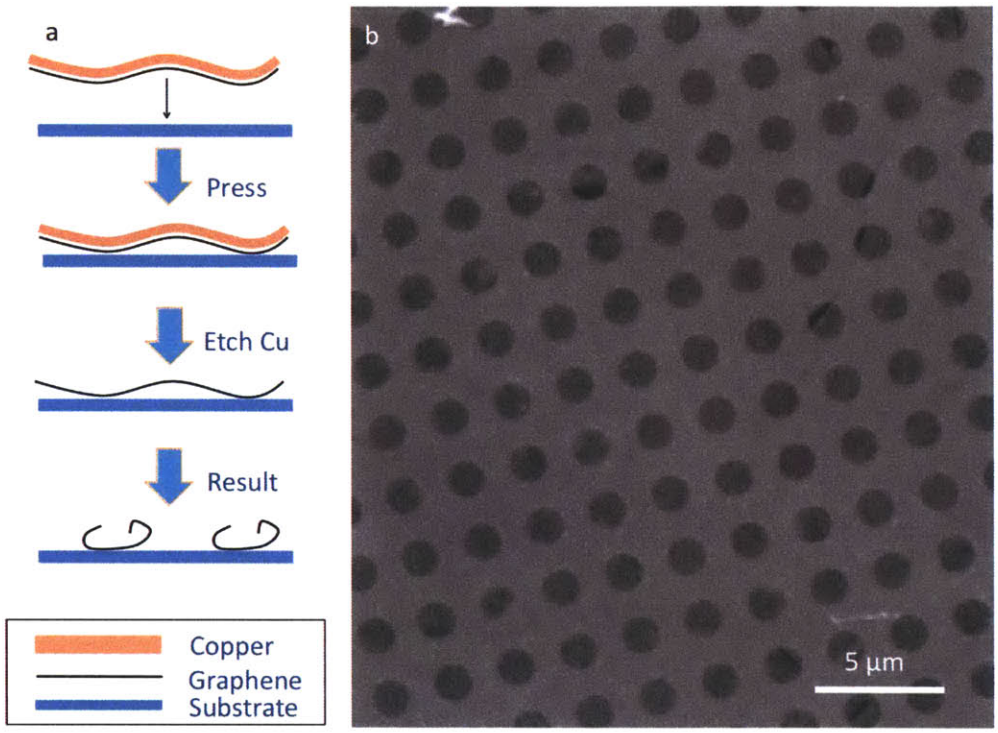

Figure 3-4: (a) Hypothesis of defect generation in graphene. Nonconformal substrate does not support graphene at all points. This leads to cracks during transfer due to surface tension pulling on unsupported portions of graphene. (b) Graphene dried in critical point drier. Much lower density of cracks as compared to other samples (see Figure 3-3).

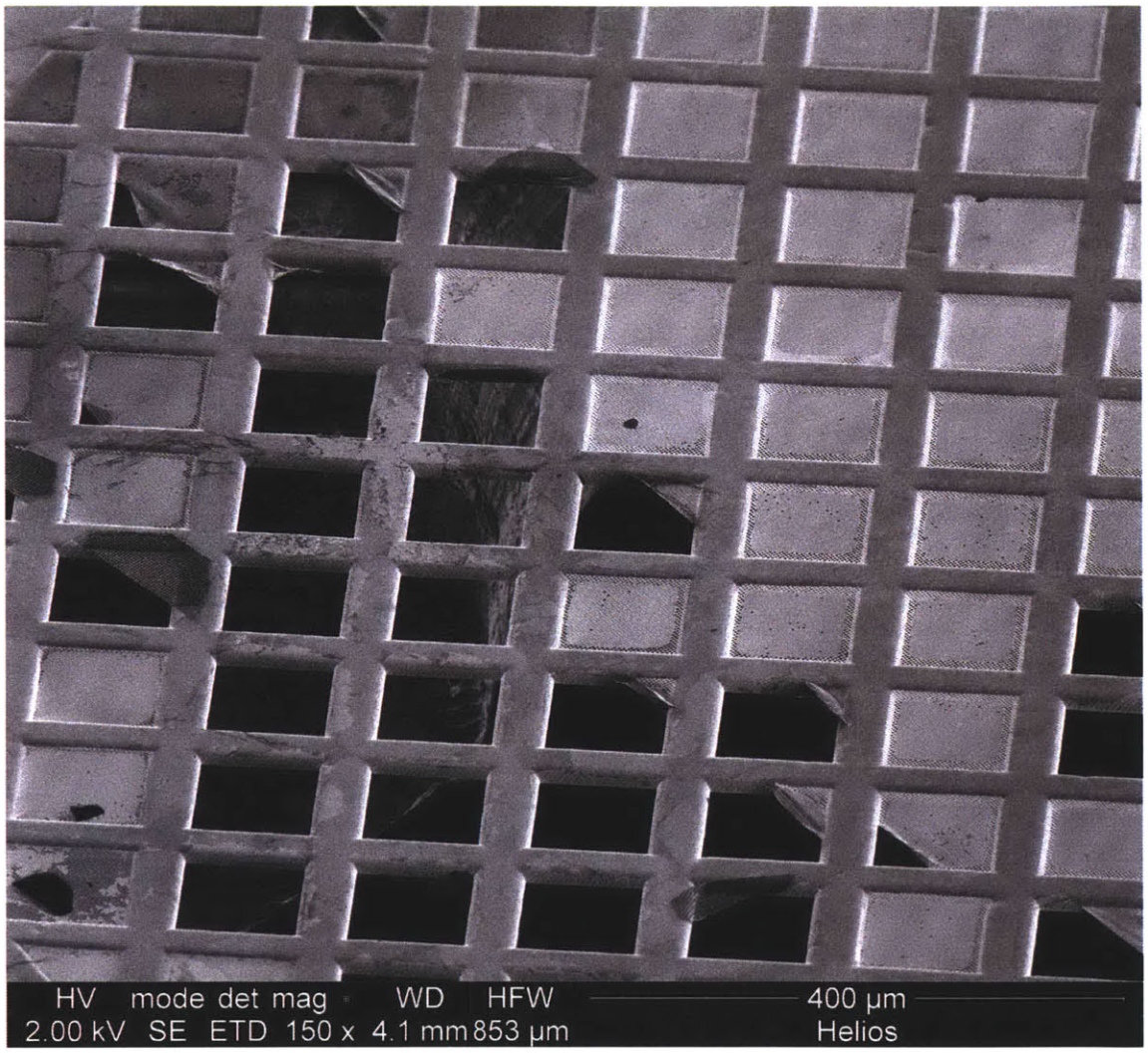

Figure 3-5: Graphene transferred to a TEM grid after final ethanol rinse. Left side of TEM grid in this image was dipped under ethanol, while right side was not. The ethanol wetting the topside of the TEM grid dislodges the amorphous carbon film from the gold grid, resulting in a poor transfer.

imaging, and Raman spectroscopy (see Figure 3-6).

The diffraction pattern of a typical TEM-supported graphene sample was imaged in a JEOL 2010F high-resolution TEM (HRTEM) at the Center for Materials Science and Engineering Electron Microscopy facility at MIT. The HRTEM was operated at 200 kV and a camera length of 200 cm. The hexagonal diffraction pattern of single-layer graphene is clearly displayed in Figure 3-6a. With this instrument, it was difficult to acquire reasonable images of the graphene because it had to be operated at 200 kV which damages the graphene lattice within a few seconds.

In order to acquire dark-field images, we collaborated with Juan-Carlos Idrobo in the Scanning Transmission Electron Microscopy Group at Oak Ridge National Laboratory through the Shared Research Equipment (SHaRE) User Facility Program and imaged our graphene in a Nion UltraSTEM 200 aberration-corrected STEM. This instrument has an point-to-point resolution of 0.8 $\AA$ when operated at 60 kV, a potential well below the knock-on energy for carbon atoms in graphene [36]. Before imaging the sample, the graphene was heated for 20 h at 160°C under vacuum to reduce the occurrence of volatile hydrocarbons on the surface of the graphene. After heating, the sample was cooled to room temperature. An image of the honeycomb graphene lattice is displayed in Figure 3-6b.

Even with heating to remove the volatile hydrocarbons a great deal of contamination was still present on our graphene (see Figure 3-6c and d). This is most likely due to volatile polymers in the oven used during the transfer process. This contamination made it difficult to determine the quality of the graphene over a large scale.

Additionally, the contamination affected the Raman spectrum of the sample. Figure 3-7a displays the Raman spectrum of our graphene sample, acquired from a WiTEC Conformal Raman Microscope, laser wavelength of 532 nm, at the Center for Nanoscale Systems at Harvard University. As shown, the graphene appears to be single layer, but with a very large D-band. The D-band is associated with defects in the graphene lattice. However, it is also associated with polymer contamination [37]. The high level of surface contamination is most likely the cause of the high D-band. To verify this assumption, another graphene sample was transferred using the above

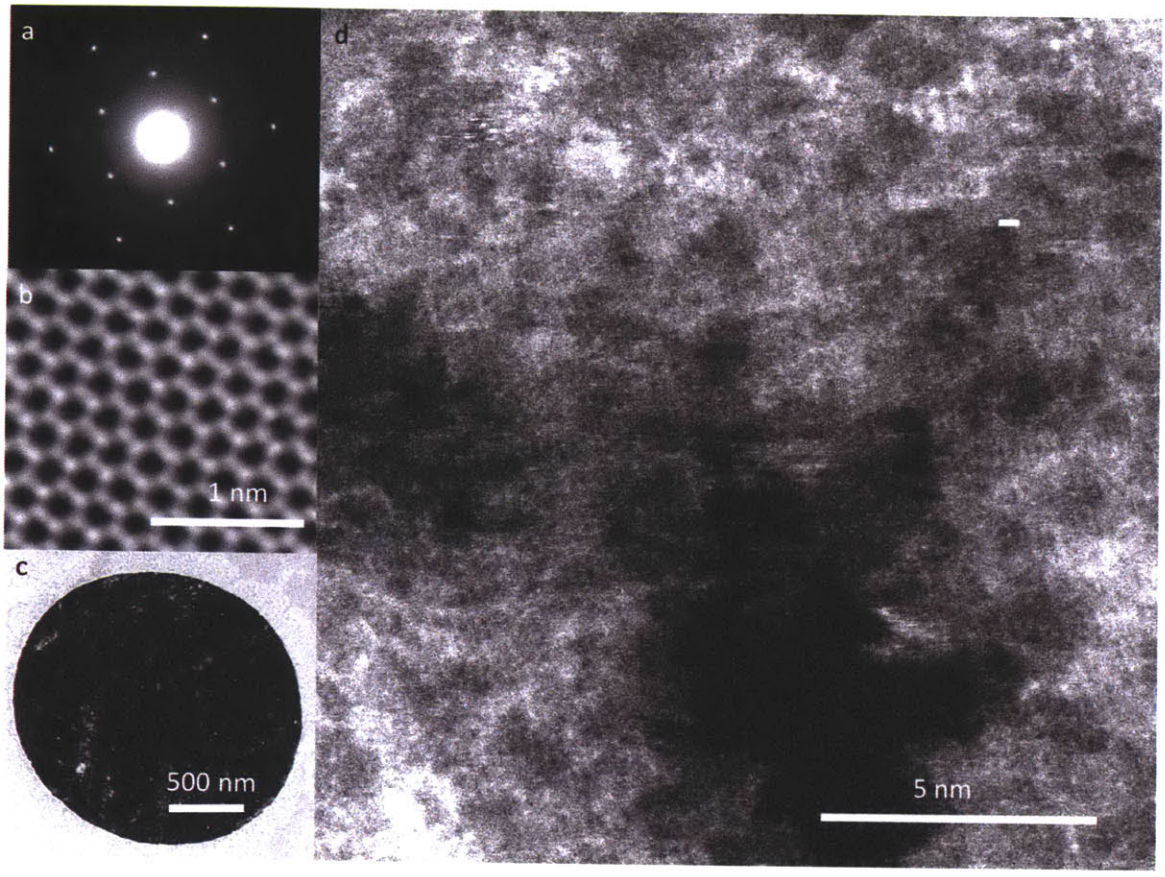

Figure 3-6: (a) Diffraction pattern of sample shows single-layer graphene. (b) Dark field scanning transmission electron microscope (STEM) image of graphene lattice. (c) Dark field STEM image of graphene suspended over pore in Quantifoil Holey Carbon TEM grid. (d) STEM dark field image showing polymer contamination on the surface of the graphene.

procedure, but without heating in the oven. The Raman spectrum for this sample is displayed Figure 3-7b. As shown, the sample has a much lower D-band signal, supporting our hypothesis.

3.3 Transfer of graphene to polycarbonate track etch membranes

Graphene on a TEM grid provides an excellent substrate for characterization. However, due to the rough topography of the TEM surface, the graphene typically has

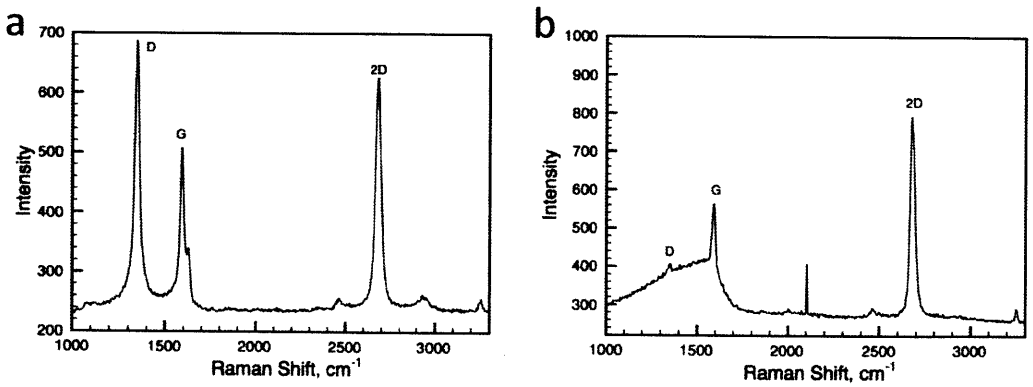

Figure 3-7: (a) Raman spectrum of suspended graphene on TEM grid. High D-band attributed to polymer contamination on the sample. Laser wavelenth was 532 nm. (b) Raman spectrum of suspended graphene on TEM grid transferred without placing in oven. Decreased D-band suggests polymer contamination occurred on the first sample during heating step.

many tears. Additionally, the size and structure of the TEM grid make it difficult to integrate it into a flow cell. Therefore, we chose a different substrate upon which to transfer the graphene in order to measure transport.

Since the lack conformality of the TEM substrate was producing tears in the graphene, the primary required characteristic of the new membrane was conformality. A conformal substrate would mitigate the effect of rough copper. Additionally, the membrane must have monodisperse and easily definable pores. This would reduce the effect of cracks on transport measurement by increasing the effective resistance of the supporting substrate.

The supporting substrate we selected was the Sterlitech polycarbonate track etch membrane with 200 nm pores. These membranes are 10 μm thick with a pore density of 3×10^8 pores/cm^2. Additionally, they have been successfully integrated into microfluidic devices in recent literature [38, 39].

3.3.1 Process

Glass slide preparation

One of the primary concerns of the transfer is keeping the PCTEM from adhering to any surface except the graphene. Adherence to other surfaces might possible pull the PCTEM away from the graphene and generate defects. Consequently, the glass slides used in this procedure were silanated for 10 min with chlorotrimethylsilane to decrease the surface energy of the glass. The resulting slide tended to increase the efficacy of the transfer by ensuring little adherence between the PCTEM and the glass slides during the pressing procedure.

Bonding procedure

After preparing the graphene and the glass slides, the graphene was bonded to the PCTEM by a simple pressing procedure. First, a ~5 mm × 5 mm copper foil with graphene was placed on a piece of weigh paper which was in turn sitting on a glass slide. A PCTEM was then placed smooth-side-down on top of the graphene. Next, another glass slide was placed on top of the PCTEM. To conform the PCTEM to the graphene, a glass pipet tube was rolled back and forth over the top glass slide under moderate finger pressure. The pressing conforms the PCTEM to the contours of the graphene, adhering it to the graphene surface. After pressing, the top glass slide was carefully removed, carrying with it the PCTEM and copper foil with graphene. To remove the PCTEM with the graphene from the glass slide, the PCTEM with the graphene was lightly placed over the top of a thin film of DI water sitting atop a third glass slide. The surface tension from the DI water gently pulls the PCTEM with the graphene off the silanated glass slide and permits it to float on the surface. Finally, the PCTEM with the graphene was transferred to the copper etchant (either CE-100 or APS-100), where the copper was etched for 1.5 h. After etching, the PCTEM-supported graphene was transferred to two subsequent DI water baths to rinse the etchant, then air-dried. Figure 3-8 displays a schematic of the transfer procedure.

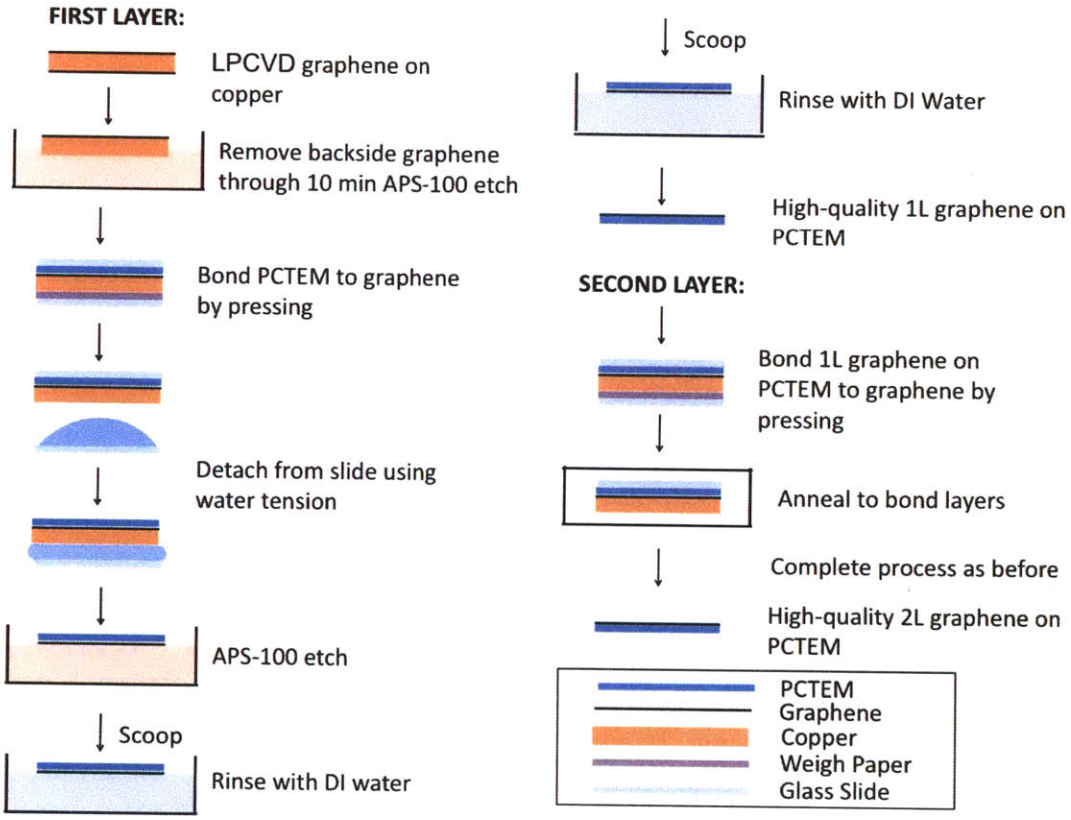

Figure 3-8: LPCVD graphene transfer process from copper foil to polycarbonate track etch membrane.

3.3.2 Parameters of transfer and impact on results

Hydrophobicity of substrate

Polycarbonate is naturally hydrophobic. Therefore, in order to ease the filling of the pores, many PCTEM manufacturers coat the surface with the wetting agent polyvinylpyrrolidone (PVP). To determine which membrane would provide the best results, we followed the above prescribed procedure and attempted to transfer graphene to both types.

The PVP-coated and PVP-free membranes behaved very differently once placed on the DI water surface. The DI water wetted the interface between the PVP-coated membrane and the graphene almost instantaneously, while the interface between the PVP-free membrane and the graphene remained dry (see Figure 3-9). This resulted in the graphene separating from the PVP-coated PCTEM surface. Therefore, the PVP-coated PCTEM was eliminated as an option as a porous support.

The PVP-free PCTEM with the copper-supported graphene was transferred from the DI water bath to the copper etchant CE-100 and etched for 1 h at room temperature and pressure, then was rinsed in two DI water baths and air dried. Figure 3-10 displays the results of the transfer. As shown, the graphene had many cracks in the surface.

Graphene topography

These cracks could have existed before the transfer or could have been generated during the transfer. To determine if these cracks existed before the transfer, we captured an SEM image of the as-synthesized graphene on copper. As Figure 3-11 shows, wrinkles in the graphene exist on the copper. This is due to the differing thermal expansion coefficients of copper and graphene, copper being 17 μm/m·K and graphene being -7 μm/m·K. During the cooling process after the graphene is synthesized, the graphene expands while the copper contracts. This leads to these wrinkles, or raised areas of graphene. Li et al. showed that these wrinkles transfer with the graphene to silicon wafers [5]. Although these wrinkles are not cracks, they

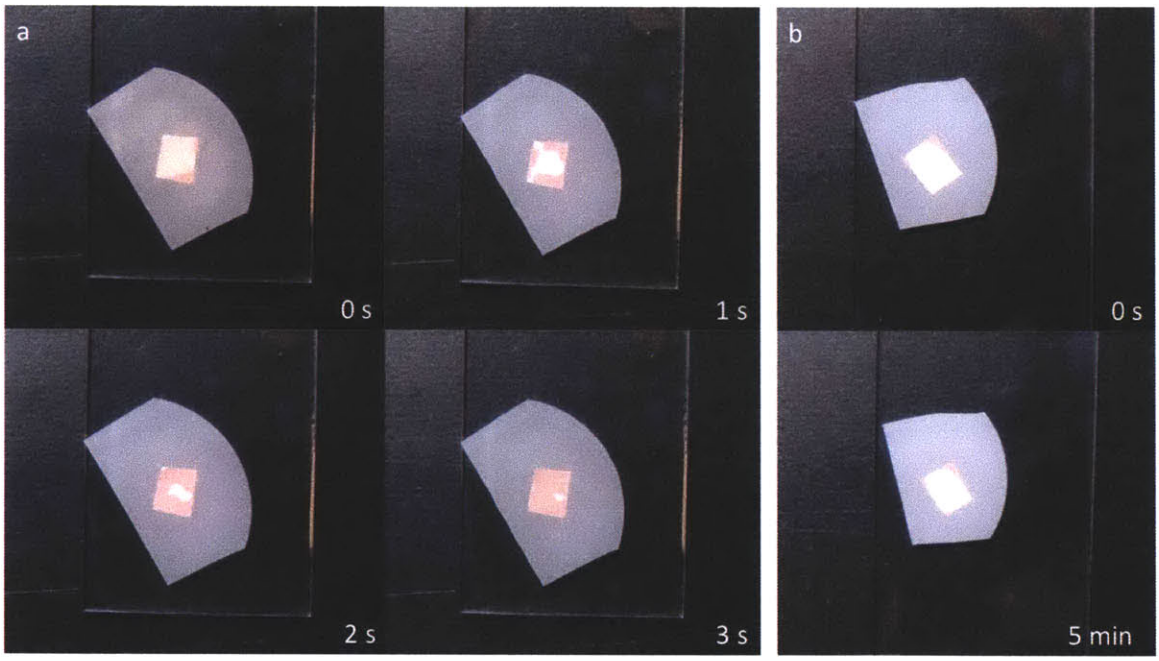

Figure 3-9: (a) Attempted transfer of graphene to polycarbonate track etch membrane (PCTEM) coated with the wetting agent PVP. Water wets surface between graphene and PCTEM completely within 5 s. (b) Transfer of graphene to PCTEM without PVP. Water does not wet surface between graphene and PCTEM. 1" x 3" glass slide is visible in images for reference.

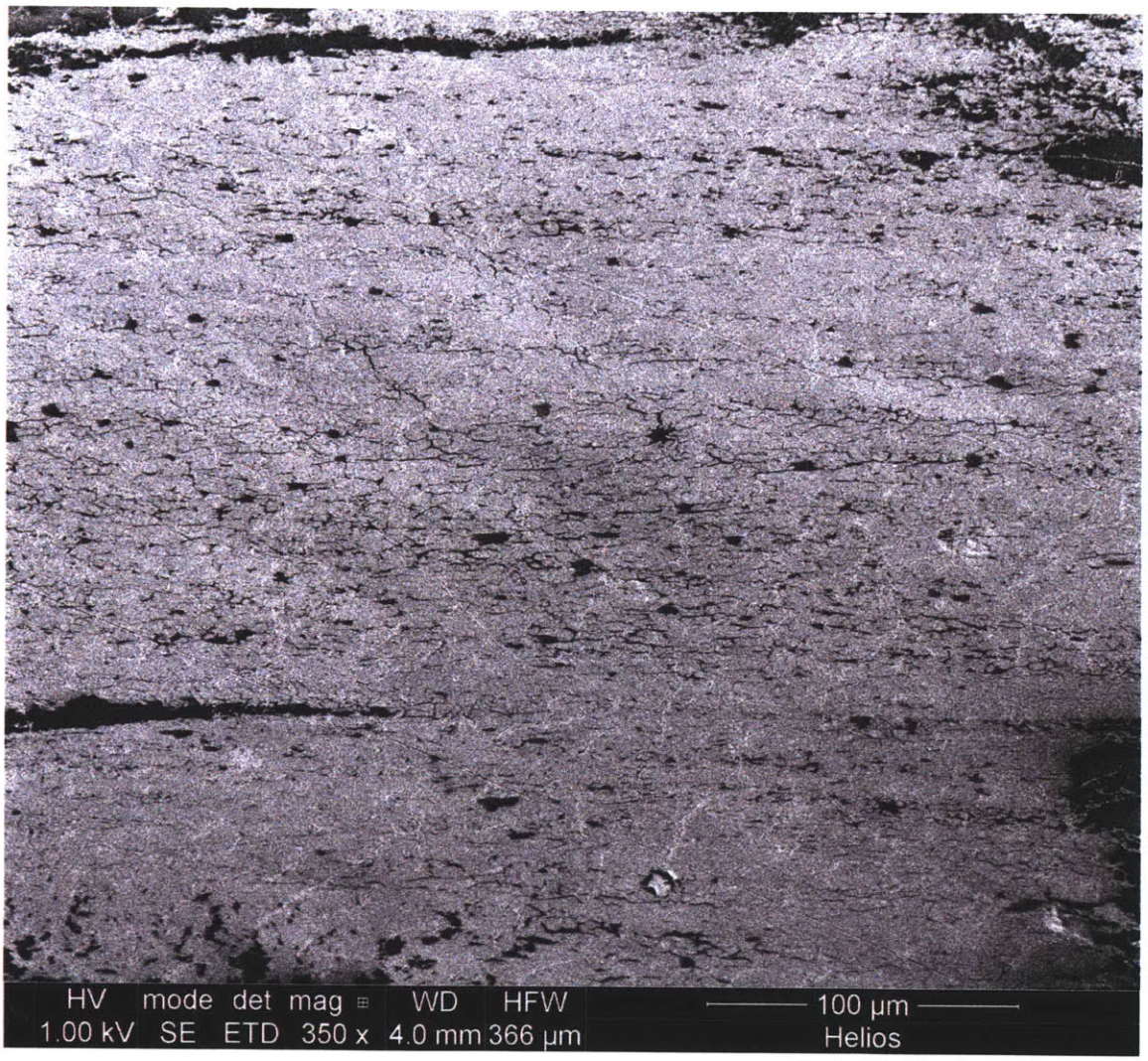

Figure 3-10: Initial graphene transfer to hydrophobic polycarbonate track etch membrane with 200 nm pores.

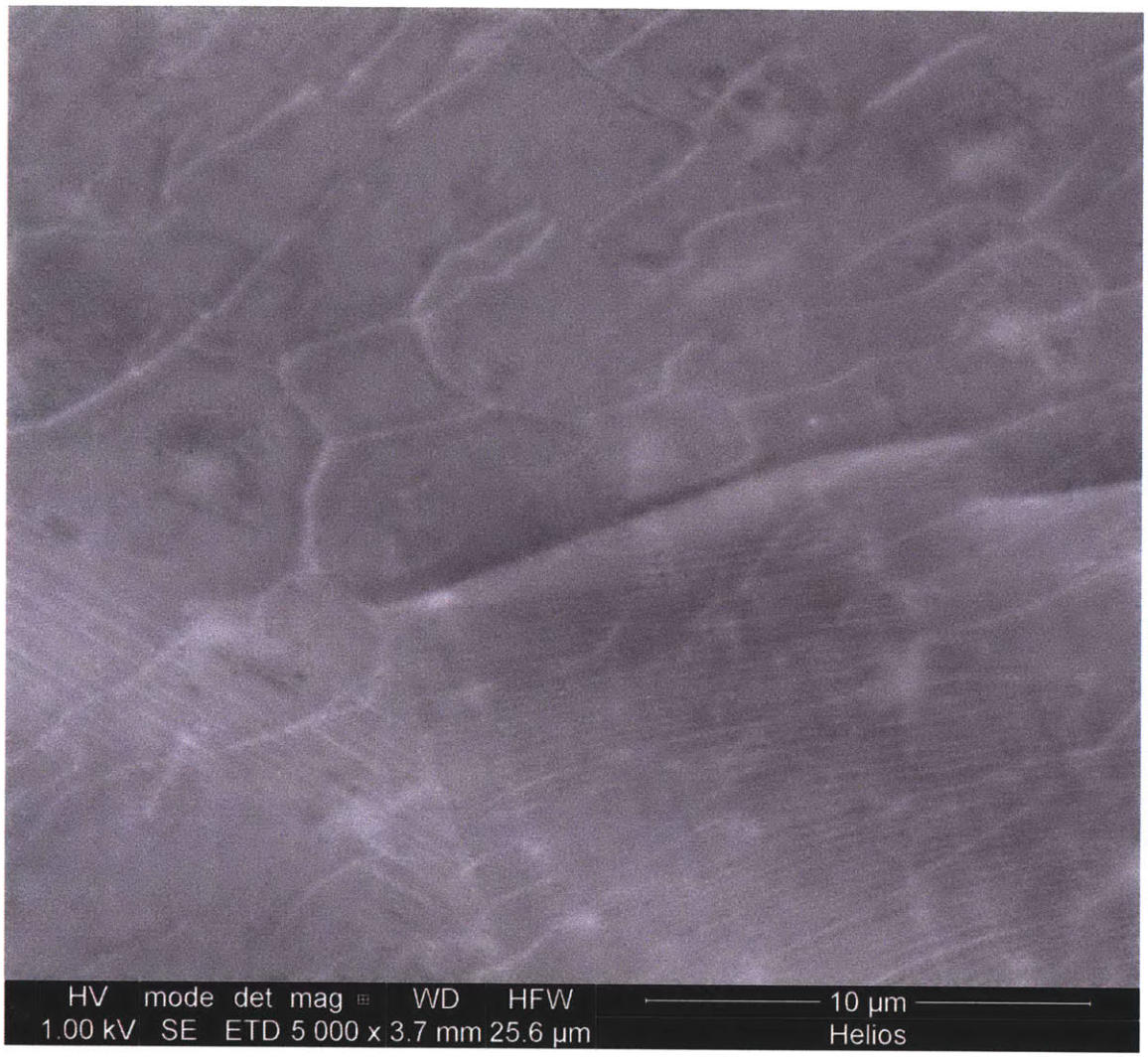

Figure 3-11: Graphene wrinkles on copper created during the contraction of the copper during cooling after graphene synthesis.

may generate cracks during transfer process.

Copper etchant

To determine the effect of the etchant on the graphene, we placed a small drop of CE-100 on the as-synthesized graphene on copper and let it etch for a few seconds. We then rinsed the membrane several times with DI water and imaged in an SEM. The results are displayed in Figure 3-12. From the image, it is clear that the products of the etching reaction, copper(I) and copper(II) chloride, are less dense than the copper

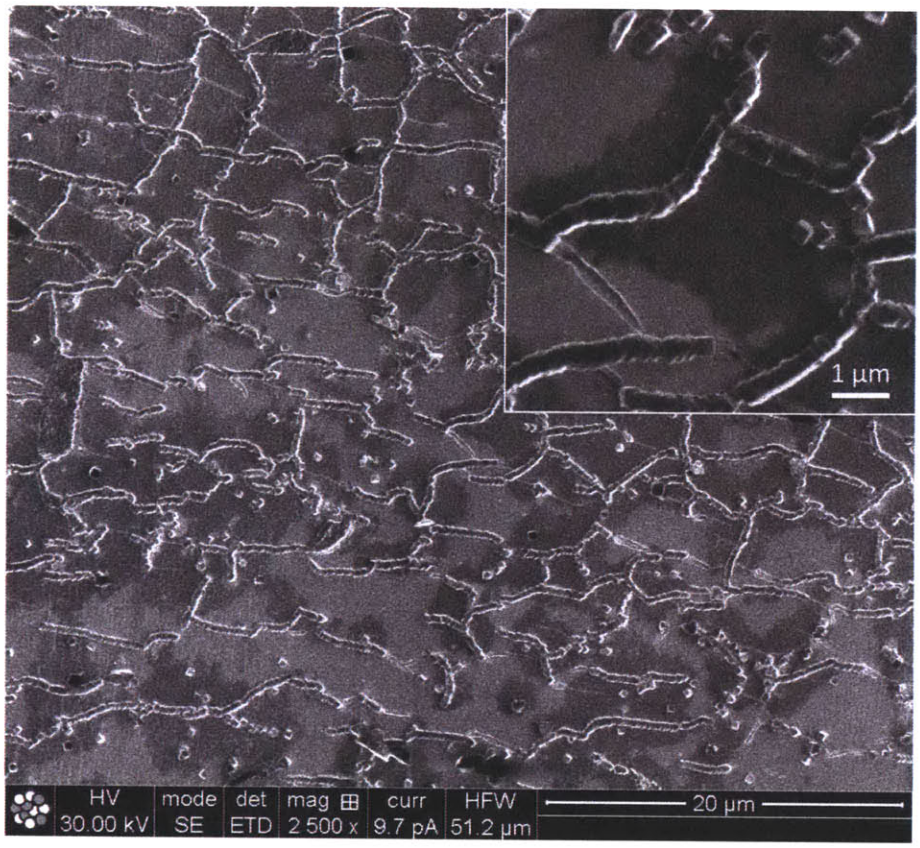

Figure 3-12: Graphene on copper after being exposed to CE-100 copper etchant. Product of reaction is less dense than copper, creating lines of reacted areas with the copper under the graphene. Inset displays crack in graphene formed from strain introduced by the crystals formed from the etching reaction.

itself. This density difference leads to strain, and ultimately tears, in the graphene as shown in the inset. Additionally, CE-100 appears to etch the copper under the grain boundaries before etching the copper under the basal plane. This may be due to the presence of defects at the grain boundaries, which initiates the crack, and possibly the reduced strength of the graphene at the grain boundaries, which provides a line of weakness for the crack to propagate [40].

One way to decrease the occurrence of cracks due to this reaction is to increase the rate of diffusion of the products of the reaction by diluting the etching solution. In this diluted solution, the products of the reaction diffuse away from the surface before they induce strain on the graphene. To accomplish this, we used a diluted

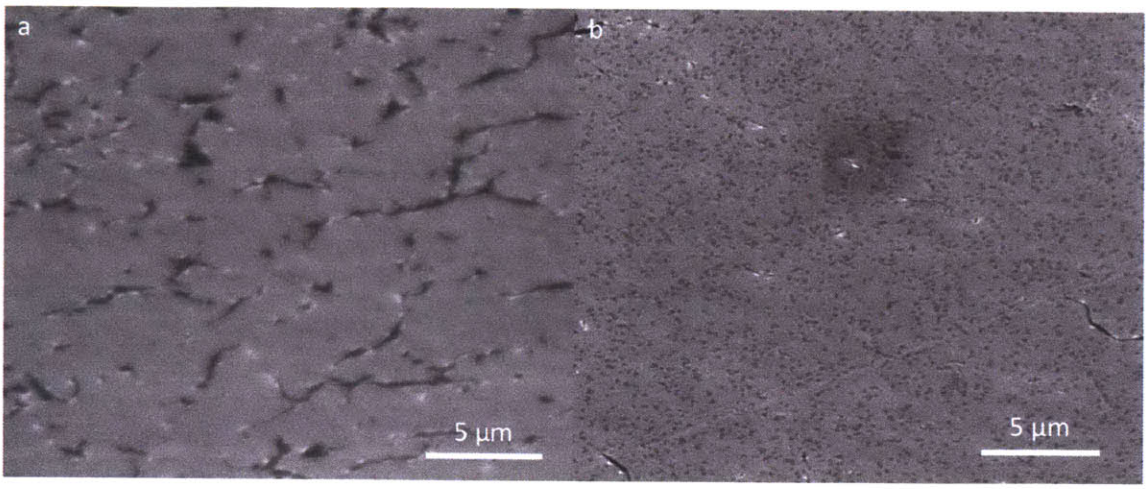

Figure 3-13: Polycarbonate track etch membrane transfer of graphene etched using (a) standard CE-100 etchant (~250 mg/mL $FeCl_3$) concentration at 25°C and (b) dilute, 0.01 g/mL, $FeCl_3 \cdot 6H_2O$ at 45°C.

ferric chloride-based etchant, 0.01 g/mL $FeCl_3 \cdot 6H_2O$, compared to the original CE-100 $FeCl_3$ concentration of 0.25-0.35 g/mL, and stirred and etched at 45°C. As shown in Figure 3-13, use of a diluted etchant reduced the occurrence of cracks in the transferred graphene.

Another way to mitigate this effect is to switch etchants, thereby changing the chemical reaction occurring at the surface. We switched etchants to APS-100 (active ingredient of ammonium peroxydisulfate). This etchant oxidizes the copper to copper(II) sulfate [41], leading to a much gentler etching procedure, and thereby higher quality transfers.

Copper topography

Although switching etchants reduced the occurrence of cracks, significant cracking events were still apparent in the transferred graphene (see Figure 3-14). Many of these cracks occurred in lines in the graphene spaced approximately the same distance apart as the troughs in the copper surface. Therefore, we hypothesized that the lines in the transferred graphene were a direct result of the surface roughness of the copper, measured to have an RMS mean value of 500 nm. In an attempt to acquire smoother

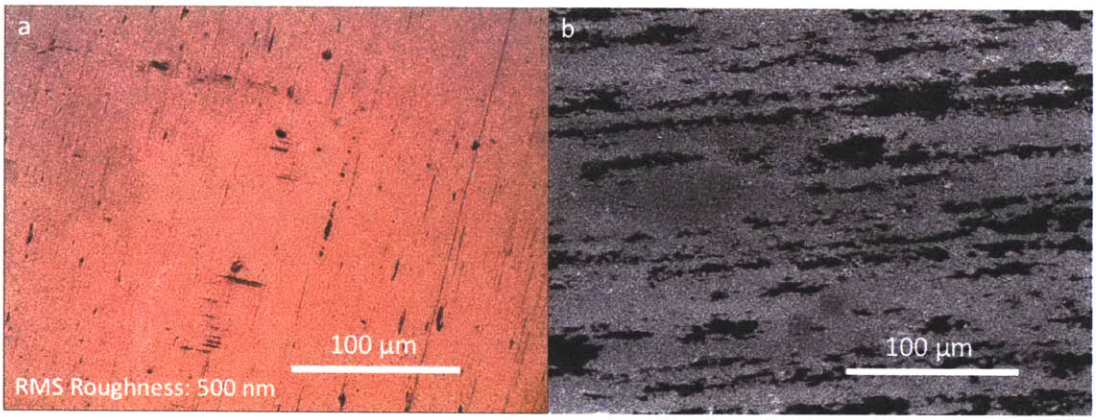

Figure 3-14: (a) Graphene on rough copper. (b) Defective lines in the graphene are easily distinguishable on PCTEM.

graphene, we switched graphene suppliers to Graphene Supermarket. After repeating the transfer using this graphene, the occurrence of the defect lines were reduced.

Etching pressure

The final defect encountered in the PCTEM transfer were single-pore defects (see Figure 3-15. We hypothesized that these were being created by hydrogen nanobubbles formed from the reaction between the APS-100 and the copper. The pressure inside these nanobubbles can reach several MPa due to their size [42], and if attached to the surface of the graphene can puncture the graphene surface. To overcome this problem, we etched the copper at 7 psi. The increased pressure increases the solubility of the hydrogen in APS-100 by ~50%, resulting in a lower occurrence of nanobubbles and the single pore defects.

3.3.3 Second-layer graphene transfer

In order to increase the transfer coverage, a second layer of graphene can be placed on the first. After allowing to air dry, the PCTEM-supported graphene was placed on a second graphene sample with the backside pre-etched. After pressing using the

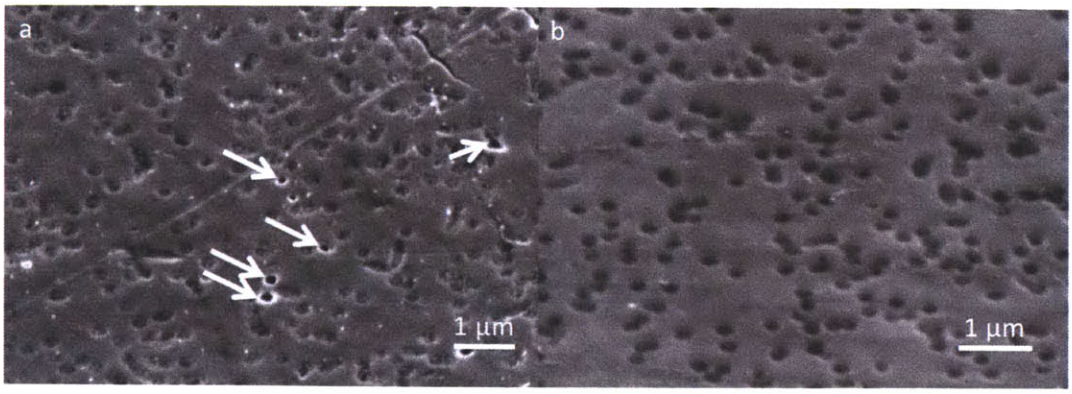

Figure 3-15: (a) Arrows point to single pore defects in graphene etched in APS-100 at atmospheric pressure. These result from insolubility of hydrogen nanobubbles created during the etching reaction. (b) Graphene etched in APS-100 under 7 psi increases solubility of hydrogen gas, resulting in few single pore defects.

same procedure as described above, the sample was placed in an oven at 140°C for 10 min to allow the pi bonds to interact, thus bonding the two layers of graphene together [43]. After cooling at room temperature, the transfer procedure was carried out as before, resulting in a double layer transfer of graphene. Figure 3-16 displays a picture of a single layer transfer and a double transfer.

3.3.4 Polycarbonate track etch membrane transfer results

Figure 3-17 is an SEM image of a typical double-layer LPCVD graphene transfer from copper foil to a PCTEM using the above procedure. The area exceeds 25 mm^2 and has no large-scale defects. In order to characterize quality of this double-layer transfer and that of a single-layer transfer, we acquired SEM images of the transferred graphene in a Helios Nanolab Dualbeam 600 at the Center for Materials Science and Engineering Electron Microscopy facility at MIT. Fifteen images were taken of the single-layer transfer and ten images were taken of the double-layer transfer and the number of broken pores counted using the particle analyzer in ImageJ64. With a median pixel value of 3 in broken pores, a cutoff threshold of 10 was used to detect broken sections. Additionally, the minimum size of the thresholded area had to be greater than 0.006 μm^2, or 20% of the total area of a pore.

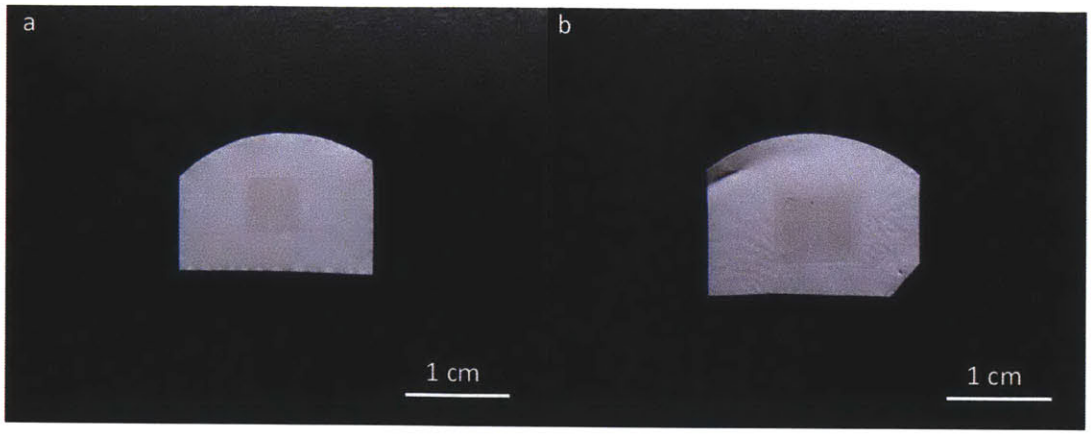

Figure 3-16: (a) Single transfer of graphene to polycarbonate track etch membrane. (b) Double transfer of graphene to polycarbonate track etch membranes.

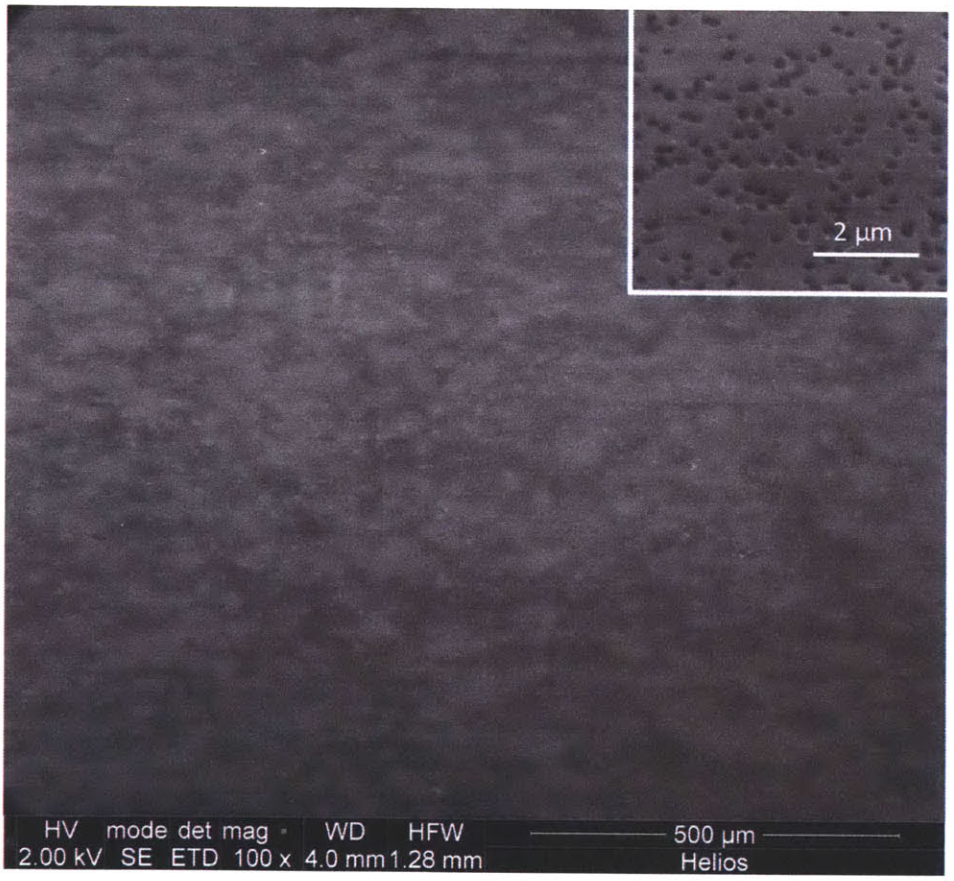

Figure 3-17: SEM image of double-layer transfer of LPCVD graphene to polycarbonate track etch membrane (PCTEM). Image confirms no large defects exist over entire 1 mm^2 area. Inset shows graphene suspended over PCTEM pores.

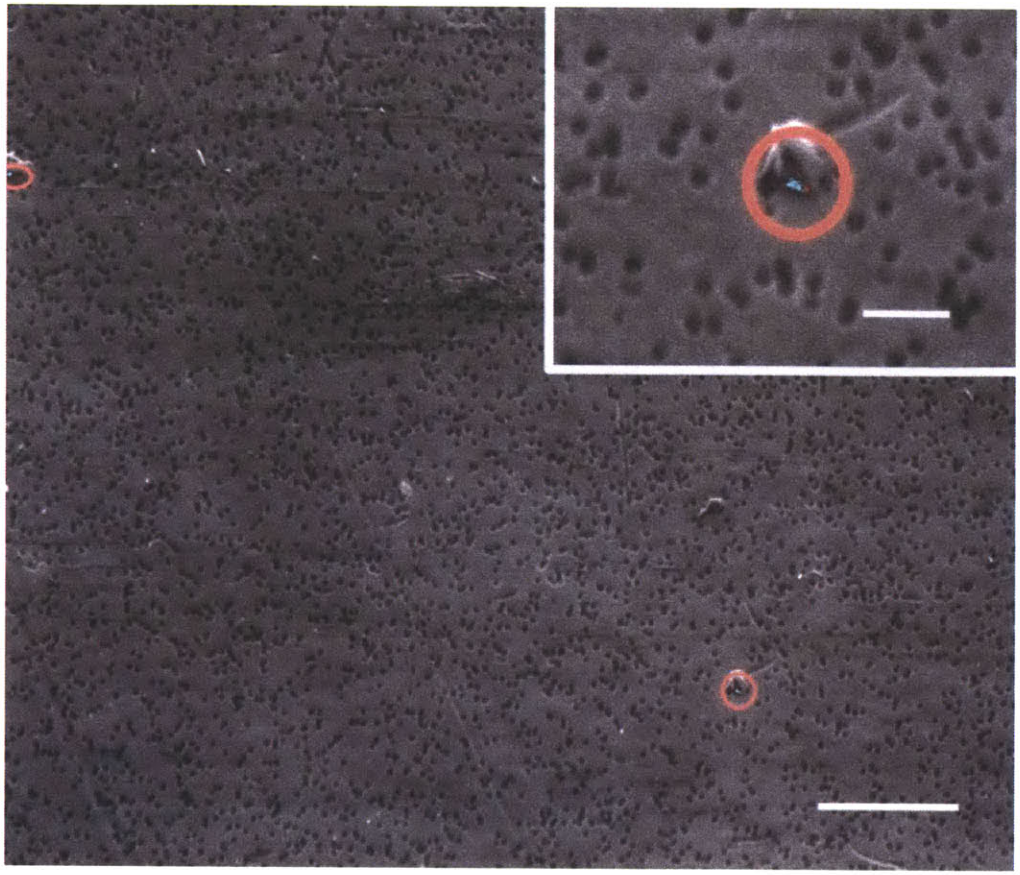

Figure 3-18: Sample thresholded image with two defects circled for clarity. Scale bar is 5 μm. Inset is zoomed in image of defect. Scale bar is 1 μm.

In the single-layer transfer, a total of 287 broken pores were counted over an area of 17257 μm^2. The PCTEM has a pore density of 3 pores/μm^2 for a total of 51772 pores. Therefore, the ratio of broken pores to covered pores is 0.0166, or a membrane quality of 98.3%. In the double-layer transfer, a total of 52 defective pores of 34392 pores were counted over an area of 11464 μm^2. The ratio of broken pores to covered pores is then 0.00454, or a membrane quality of 99.55%. Figure 3-18 displays an example thresholded image with the defects circled in the double-layer graphene transfer.

THIS PAGE INTENTIONALLY LEFT BLANK

Chapter 4

Conclusions

To address the impending water crisis, new technology must be developed that increases the efficiency of desalination processes. New nanostructured materials, such as porous graphene membranes, have the potential to this meet this need by selectively permitting a high flux of water while still rejecting the transport of salt ions. To produce such membranes, a process needs to be developed to transfer large areas of graphene to a porous support in order to study the transport properties of water and ions through these membranes.

The graphene transfer method presented in this work fulfills this need. Through our procedure, it is possible to transfer areas of LPCVD graphene exceeding 25 mm^2 of greater than 99.5% defect-free coverage to polycarbonate track etch membranes. This transfer procedure will permit the study of the passage of water and ions through pores in graphene in the coming months, thereby providing a foundation for the development of future membrane materials.

THIS PAGE INTENTIONALLY LEFT BLANK

Bibliography

[1] Comprehensive Assessment of Water Management in Agriculture. Water for food, water for life: a comprehensive assessment of water management in agriculture . Earthscan, London, 2007.

[2] K S Novoselov, A K Geim, S V Morozov, D Jiang, Y Zhang, S V Dubonos, I V Grigorieva, and A A Firsov. Electric Field Effect in Atomically Thin Carbon Films. *Science*, 306(5696):666–669, October 2004.

[3] S Park and R S Ruoff. Chemical Methods for the Production of Graphenes. *Nature Nanotechnology*, 4:217–224, March 2009.

[4] D K Gaskill, G F Jernigan, P M Campbell, J L Tedesco, J C Culbertson, B L VanMil, R L Myers-Ward, C R Eddy Jr, J Moon, D Curtis, M Hu, D Wong, C McGuire, J A Robinson, M A Fanton, J P Stitt, T Stitt, D Snyder, X Wang, and E Frantz. Epitaxial graphene growth on SiC wafers. In *215th ECS Meeting*, pages 117–124. ECS, 2009.

[5] X Li, W Cai, J An, S Kim, J Nah, D Yang, R Piner, A Velamakanni, I Jung, E Tutuc, S K Banerjee, L Colombo, and R S Ruoff. Large-Area Synthesis of High-Quality and Uniform Graphene Films on Copper Foils. *Science*, 324(5932):1312–1314, June 2009.

[6] X Liang, Z Fu, and S Y Chou. Graphene Transistors Fabricated via Transfer-Printing In Device Active-Areas on Large Wafer. *Nano Letters*, 7(12):3840–3844, November 2007.

[7] LH Liu and M Yan. Simple Method for the Covalent Immobilization of Graphene. *Nano Letters*, 9(9):3375–3378, September 2009.

[8] M J Allen, V C Tung, L Gomez, Z Xu, LM Chen, K S Nelson, C Zhou, R B Kaner, and Y Yang. Soft Transfer Printing of Chemically Converted Graphene. *Advanced Materials*, 21(20):2098–2102, May 2009.

[9] W Regan, N Alem, B Aleman, B Geng, C Girit, L Maserati, F Wang, M Crommie, and A Zettl. A direct transfer of layer-area graphene. *Applied Physics Letters*, 96(11):113102, 2010.

[10] B Aleman, W Regan, S Aloni, V Altoe, N Alem, C Girit, B Geng, L Maserati, M Crommie, F Wang, and A Zettl. Transfer-Free Batch Fabrication of Large-Area Suspended Graphene Membranes. *ACS Nano*, 4(8):4762–4768, 2010.

[11] R F Service. Desalination freshens up. *Science*, 313(5790):1088–1090, 2006.

[12] J Miller. Review of Water Resources and Desalination Technologies. *Sandia National Laboratories Report*, 2003.

[13] T Humplik, J Lee, S C O'Hern, BA Fellman, M A Baig, S F Hassan, M A Atieh, F Rahman, T Laoui, R Karnik, and E N Wang. Nanostructured materials for water desalination. *Nanotechnology*, 22(29):292001, 2011.

[14] L F Greenlee, D F Lawler, B D Freeman, B Marrot, and P Moulin. Reverse osmosis desalination: Water sources, technology, and today's challenges. *Water Research*, 43(9):2317–2348, May 2009.

[15] S K Sahoo and V Labhasetwar. Nanotech approaches to drug delivery and imaging. *Drug Discovery Today*, 8(24):1112–1120, December 2003.

[16] A H Lu, E L Salabas, and F Schuth. Magnetic nanoparticles: synthesis, protection, functionalization, and application. *Angewandte Chemie International Edition*, 46(8), February 2007.

[17] A S Arico, P Bruce, B Scrosati, J M Tarascon, and W Van Schalkwijk. Nanostructured materials for advanced energy conversion and storage devices. *Nature Materials*, 4:366–377, 2005.

[18] C J Murphy, T K Sau, A M Gole, C J Orendorff, J Gao, L Gou, S E Hunyadi, and T Li. Anisotropic Metal Nanoparticles: Synthesis, Assembly, and Optical Applications. *The Journal of Physical Chemistry B*, 109(29):13857–13870, July 2005.

[19] N O'Farrell, A Houlton, and B R Horrocks. Silicon nanoparticles: applications in cell biology and medicine. *International Journal of Nanomedicine*, 1(4):451–472, December 2006.

[20] C Lee, X Wei, J W. Kysar, and J Hone. Measurement of the Elastic Properties and Intrinsic Strength of Monolayer of Graphene. *Science*, 321(5887):385, July 2008.

[21] J S Bunch, S S Verbridge, J S Alden, A M Van Der Zande, J M Parpia, H G Craighead, and P L McEuen. Impermeable Atomic Membranes from Graphene Sheets. *Nano Letters*, 8(8):2458–2462, August 2008.

[22] M Lucchese, F Stavale, E H Martins Ferreira, C Vilani, M V O Moutinho, R B Capaz, C A Achete, and A Jorio. Quantifying ion-induced defects and Raman relaxation length in graphene. *Carbon*, 48(5):1592–1597, April 2011.

[23] S Mathew, T K Chan, D Zhan, K Gopinadhan, A R Barman, M B H Breese, S Dhar, Z X Shen, T Venkatesan, and J T L Thong. The effect of layer number and substrate on the stability of graphene under MeV proton beam irradiation. *Carbon*, 49(5):1720–1726, April 2010.

[24] J Bai, X Zhong, S Jiang, Y Huang, and X Duan. Graphene nanomesh. *Nature Nanotechnology*, 5:190–194, February 2010.

[25] J I Paredes, P Solís-Fernández, A Martínez-Alonso, and J M D Tascón. Atomic Vacancy Engineering of Graphitic Surfaces: Controlling the Generation and Har-

nessing the Migration of the Single Vacancy. *The Journal of Physical Chemistry C*, 113(23):10249–10255, June 2009.

[26] C Berger, Z Song, T Li, X Li, A Y Ogbazghi, R Feng, Z Dai, A N Marchenkov, E H Conrad, P N First, and W A de Heer. Ultrathin Epitaxial Graphite: 2D Electron Gas Properties and a Route toward Graphene-based Nanoeletronics. *Journal of Physical Chemistry B*, 108:19912–19916, October 2004.

[27] A K Geim. Graphene: Status and Prospects. *Science*, 324(5934):1530–1534, June 2009.

[28] J Robinson, X Weng, K Trumbull, R Cavalero, M Wetherington, E Frantz, M LaBella, Z Hughes, M Fanton, and D Snyder. Nucleation of Epitaxial Graphene on SiC(0001). *ACS Nano*, 4(1):153–158, 2010.

[29] C Riedl, C Coletti, and U Starke. Structural and electronic properties of epitaxial graphene on SiC(0001): a review of growth, characterization, transfer doping and hydrogen intercalation. *Journal of Physics D-Applied Physics*, 43(37):17, 2010.

[30] K S Kim, Y Zhao, H Jang, S Y Lee, J M Kim, K S Kim, JH Ahn, P Kim, JY Choi, and B H Hong. Large-scale pattern growth of graphene films for stretchable transparent electrodes. *Nature*, 457(7230):706–710, January 2009.

[31] J D Caldwell, T J Anderson, J C Culbertson, G G Jernigan, K D Hobart, Fritz J Kub, Marko J Tadjer, J L Tedesco, J K Hite, M A Mastro, R L Myers-Ward, Charles R Eddy Jr, P M Campbell, and D K Gaskill. Technique for the Dry Transfer of Epitaxial Graphene onto Arbitrary Substrates. *ACS Nano*, 4(2):1108–1114, February 2010.

[32] A Reina, X Jia, H Ho, D Nezich, H Son, V Bulovic, M S Dresselhaus, and J Kong. Large Area, Few-Layer Graphene Films on Arbitrary Substrates by Chemical Vapor Deposition. *Nano Letters*, 9(1):30–35, January 2009.

[33] Y Lin, C Jin, J Lee, S Jen, K Suenaga, and P Chiu. Clean Transfer of Graphene for Isolation and Suspension. *ACS Nano*, 5(3):2362–2368, February 2011.

[34] R S Pantelic, J W Suk, C W Magnuson, J C Meyer, P Wachsmuth, U Kaiser, R S Ruoff, and H Stahlberg. Graphene: Substrate preparation and introduction. *Journal of Structural Biology*, 174:234–238, October 2010.

[35] M E Suk and N R Aluru. Water Transport through Ultrathin Graphene. *The Journal of Physical Chemistry Letters*, 1:1590–1594, April 2010.

[36] F Banhart, J Kotakoski, and A V Krasheninnikov. Structural Defects in Graphene. *ACS Nano*, 5(1):26–41, 2011.

[37] J Song, T Y Ko, and S Ryu. Raman Spectroscopy Study of Annealing-Induced Effects on Graphene Prepared by Micromechanical Exfoliation. *Bulletin of the Korean Chemical Society*, 31(9):2679–2682, 2010.

[38] K Aran, L A Sasso, N Kamdar, and J D Zahn. Irreversible, direct bonding of nanoporous polymer membranes to PDMS or glass microdevices. *Lab On A Chip*, 10(5):548–552, 2010.

[39] B Chueh, D Huh, C R Kyrtsos, T Houssin, N Futai, and S Takayama. Leakage-free bonding of porous membranes into layered microfluidic array systems. *Analytical Chemistry*, 79(9):3504–3508, 2007.

[40] P Huang, C Ruiz-Vargas, A van der Zande, W S Whitney, M P Levendorf, J W Kevek, S Garg, J S Alden, C J Hustedt, Y Zhu, J Park, P L McEuen, and D A Muller. Grains and grain boundaries in single-layer graphene atomic patchwork quilts. *Nature*, 469:389–393, January 2011.

[41] K R Williams, K Gupta, and M Wasilik. Etch rates for micromachining processing - Part II. *Journal of Microelectromechanical Systems*, 12(6):761–778, 2003.

[42] S Yang, S M Dammer, N Bremond, H J W Zandvliet, E S Kooij, and D Lohse. Characterization of nanobubbles on hydrophobic surfaces in water. *Langmuir*, 23(13):7072–7077, 2007.

[43] Y Wang, S W Tong, X F Xu, B Ozyilmaz, and K P Loh. Interface Engineering of Layer-by-Layer Stacked Graphene Anodes for High-Performance Organic Solar Cells. *Advanced Materials*, 23(13):1514–1518, 2011.